CHAPTER 1

INTRODUCTION

Hydrated salts are ionic compounds that trap water molecule within their crystal structure as they crystallize. The water molecules are called the water of hydration. When the salt hydrate gets heated it is converted to its anhydrous form or to a salt hydrate with fewer moles of water. There is a lot of significance in much undiscovered area of salt hydrates. The study of salt hydrates helps us to discover new areas and new options in scientific research.

Phase change of salt hydrate is a challenging area is the. Currently the society and countries are moving toward more energy efficient and energy saving methodologies. The study of salt hydrates helps us to contribute towards these efforts. A dominant part of the European and Western parts use electricity from nonrenewable resource for domestic heating and hot tap water generation. A promising heat storage method and use the stored whenever required can be provided by developing salt hydrate as heat storage concept based on thermochemical reactions. Thereby dependence on nonrenewable sources can be reduced. [1-3]

The study preformed also helps us to analyses salt prediction sequence and thereby helps in designing chemical engineering process to extract valuable salts from salt lake brine economically and efficiently. The aqueous phase and salt phase of various salts were studied. [2-10]

The salt hydrates have few industrially attractive properties such as: (1) high latent heat of phase change per unit volume, (2) relatively high thermal conductivity (almost double that of paraffin waxes), (3) small volume change on dehydration and hydration, (4) compatibility with many thermoplastics, and (5) non-toxicity. Many salt hydrates are sufficiently inexpensive for use in thermal storage. Many researchers have studied the compounded eutectic hydrate salt to achieve more suitable phase change temperature and better cold storage performance.

Furthermore, It has been widely used in solar energy storage, industrial waste heat utilization, building heating and air conditioning, thermal management of mobile devices, and so on. The traditional ice storage and water storage cannot reach the temperature of low-temperature cold storage. The temperature requirement of low cold storage is between −20 and −30°C, and the high-temperature cold storage is between 0 and 4°C. However, the ice storage and water storage systems can only reach 0°C, which cannot meet the requirements of the low-temperature application. Adding inorganic salts in the water can ensure that the amount of phase change latent heat almost unchanged and reduce the phase change temperature of the storage material at the same time. Compound salts can not only further reduce the melting point of solidification but also optimize and modify the overall physical properties of certain materials. However, notable disadvantages of salt hydrates limit their application in thermal insulation composites. The major difficulty of using salt hydrates as PCMs is their incongruent or semi-congruent melting.[20-30]

Contrary to the congruent dehydration (melting) behavior of hydrated salts, which occurs if the anhydrous salt is entirely soluble in its water of hydration at the melting temperature, in incongruent and semi-congruent melting the amount of water separated from the hydrated salt is not sufficient to dissolve the salt crystals. Therefore, the resulting mixture becomes supersaturated, and the salt crystals segregate from the water phase. As a result of this phase segregation, recombination of salt with water of crystallization becomes unachievable during freezing. This irreversible dehydration causes the loss of thermal effectiveness of the hydrated salt on thermal cycling. Other disadvantages of hydrated salts are difficulty in crystal nucleation and experiencing supercooling, and corrosiveness[31-55]

Apart from aforementioned problem, the storage capacity depends on the volume-specific enthalpy of melting. At temperatures below 423 K, the most significant values are found for salt hydrates. Therefore, the technical literature is rich in proposals of heat storage applications for salt hydrates. However, for practical performance besides the heat storage capacity, appropriate melting–

crystallization temperatures within a few degrees are crucial for intended applications. Also, reversible phase changes over many heating–cooling cycles have to be ensured, which is easier with congruent melting than with incongruent melting hydrates. Also, most of the salt hydrates are incongruently melting, which requires technical measures to reach hydration equilibrium. Knowledge of the solid–liquid equilibria represents the most important presumption for systematic evaluations of the suitability of salt mixtures. Unfortunately, there are only a few detailed experimental investigations of such phase diagrams. Due to the tendency of salt hydrates for supercooling, experimental determinations of liquidus curves are time-consuming. Therefore, it has been decided to develop a suitable thermodynamical model for phase analysis of salt hydrate well as validating the result with experimental data for solid-liquid phase diagram determinations.

1.2 Objectives of the Study

The main objectives include:

1. Study of Charging and Discharging cycles
2. Study of Capacity of batteries
3. Study of thermal management in batteries

CHAPTER 2

LITERATURE REVIEW

M. Gaeini (2018) studied that thermochemical heat storage in salt hydrates is a promising method to improve the solar fraction in the built environment. The major concern at that stage is liquefaction followed by washing out of active material and agglomeration into large chunks of salt, thus deteriorating the diffusive properties of the porous salt hydrate structure. In his work, specific attention is given to the methods to stabilize a sample salt hydrate. Attempts have been made to stabilize calcium chloride by impregnation in expanded natural graphite and vermiculite, and by microencapsulation with ethyl cellulose. The effect of these stabilization methods on the performance of the material, such as kinetics and energy density, has investigated. Characterization of the materials is carried out with combined Thermo-Gravitational Analysis (TGA) and Differential Scanning Calorimetry (DSC) methods and microscopic observation, in order to evaluate the improvements on the basis of three subjects: reaction kinetics, heat storage density and stability

Calcium chloride is found to be one of the promising salt hydrates for thermochemical heat storage for common building applications. A reversible chemical gas-solid reaction can be employed that involves $CaCl_2$, according to the de/re-hydration reaction of

$$CaCl_2 \cdot H_2O(s) + heat \rightleftarrows \ CaCl_2 \cdot (x-y)H_2O(s) + yH_2O\ (g)$$

The interest for calcium chloride has been triggered by: easy availability and subsequently low price, high capacity for water uptake and energy storage density, relatively better chemical stability than other salt hydrates, low

corrosiveness and non toxicity. Furthermore, the material dehydrates at low temperature (below 100 °C), which makes it suitable for the applications.

The energy storage density is studied for the four calcium chloride based materials. The energy release for each sample during hydration from anhydrous to hexahydrous state was studied. The simultaneous thermal analysis method allows the estimation of the energy per mole of calcium chloride and per mole of absorbed water. Microencapsulated calcium chloride showed high multicyclic stability, compared with pure and impregnated materials, that liquefy upon hydration under the given conditions. Microencapsulated material remains stable over multiple cycles and shows the fastest kinetics. The only disadvantage of the encapsulation methodology used in paper is the resulting low energy storage density.

Ard-Jan de Jong (2016) observed that long-term and compact storage of solar energy is crucial for the eventual transition to a 100% renewable energy economy. For that, thermochemical materials provided a promising solution. The compactness of a long-term storage system was determined by the thermochemical reaction, operating conditions, and system implementation with the necessary additional system components. Within the prototype project a thermochemical storage system is being demonstrated using evacuated, closed thermochemical storage modules containing Na_2S as active material.

A significant part of energy to be stored is for space heating and domestic hot water for buildings. Daily storage can be arranged by mature boiler technology, but seasonal storage for at least half a year will require considerably lower heat losses. Besides, seasonal heat storage will usually imply storing very large amounts of heat, so that heat storage should be compact, with high storage density. Energy storage by using solar heat (e.g. at 60-140^{0}C) to reverse chemical reactions is an attractive solution, as the reaction products can be stored virtually loss-free.

Thermochemical storage offers the potential of loss-free storage with a heat storage density higher than water. The first lab results of the prototype used in this project showed that a storage density of 0.14GJ/m^3 was achieved and they observed that it can expect to reach 0.18GJ/m^3 for coming field tests. In this paper identified and analyzed several possible improvements and show that by mere optimization of the prototype fixed-bed reactor concept using Na_2S, a heat storage density of approximately 1GJ/m^3 can already be achieved.

Michael Graham(2016) studied that thermal energy storage has many important applications, and is most efficiently achieved by latent heat storage using phase change materials (PCMs). Salt hydrates have advantages such as high energy storage density, high latent heat and incombustability. However, they suffer from drawbacks such as incongruent melting and corrosion of metallic container materials. By encapsulating them in a polymer shell, problems can be eliminated. Here we demonstrate a simple method to nanoencapsulate magnesium nitrate hexhydrate, employing an in situ mini emulsion polymerisation with ethyl-2- cyanoacrylate as monomer. Using sonication to prepare mini emulsions improved the synthesis by reducing the amount of surfactant required as stabiliser. Thermal properties were analysed by differential scanning calorimetry (DSC) and thermogravimetric analysis (TGA). Fourier transform infrared spectroscopy (FTIR) was employed to prove the presence of salt hydrate within the nanocapsules. Results showed the capsules are 100-200nm in size, have salt hydrate located in the core and are stable over at least 100 thermal cycles with only a 3% reduction in latent heat. Supercooling is also drastically reduced

DSC results demonstrated for the first time high thermal stability of the nanoencapsulated salt hydrates, which remained unchanged after 100 thermal cycles with a latent heat of 83.2Jg^{-1}. Chemical and macroscale stability of the nanoencapsulated salt hydrates were also proven by FTIR and visual observations after heating/cooling cycles. The thermal properties of the nanocapsules are a

great improvement over the bulk $Mg(NO_3)_2 \cdot 6H_2O$, which loses its structural integrity and chemical composition after only 5 cycles.

Salt hydrate PCMs with long lifetimes are important for future energy storage applications, due to their high heat capacity and cost effectiveness compared to commonly used paraffin wax PCMs. Efficient energy storage has the potential to greatly reduce global energy demand, providing a sustainable future

Lin Liang (2017) studied that a new cold storage phase change material eutectic hydrate salt ($K_2HPO_4 \cdot 3H_2O$–$NaH_2PO_4 \cdot 2H_2O$–$Na_2S_2O_3 \cdot 5H_2O$) was prepared, modified, and tested. The modification was performed by adding a nucleating agent and thickener. The physical properties such as viscosity, surface tension, cold storage characteristics, supercooling, and the stability during freeze-thaw cycles were studied. Results showed that the use of nucleating agents, such as sodium tetraborate, sodium fluoride, and nanoparticles, are effective. The solidification temperature and latent heat of these materials which was added with 0, 3, and 5 wt% thickeners were −11.9, −10.6, and −14.8° C and 127.2, 118.6, 82.56 J/g, respectively. Adding a nucleating agent can effectively improve the nucleation rate and nucleation stability. Furthermore, increasing viscosity has a positive impact on the solidification rate, supercooling, and the stability during freeze-thaw cycles.

Luca Scapino (2017) studied that sorption heat storage has the potential to store large amounts of thermal energy from renewables and other distributed energy sources. This article provides an overview on the recent advancements on long-term sorption heat storage at material- and prototype- scales. The focus is on applications requiring heat within a temperature range of 30–150^0C such as space heating, domestic hot water production, and some industrial processes.
Thermal energy storage is an attractive storage category because in principle it can be more economical than other technologies, it has a wide range of storage possibilities with storage periods ranging from minutes to months, and finally

because thermal energy dominates the final energy use in sectors such as industry or household .Thermal energy storage can be divided into three main categories according to how energy is stored: sensible heat (e.g. water tanks, underground storage) latent heat (e.g. ice, phase change materials) , and sorption heat storage

Currently, composite materials are investigated because they have the potential to overcome the disadvantages of pure salt hydrates by increasing their hydrothermal stability. This is done by mixing or impregnating salt hydrates with highly porous host matrices or powders. However, problems in heat and mass transport still can arise due to the reduction of empty pores, possible deliquescence and leakage of the salt from the composite, and degradation. To this regard, further research is needed to overcome these problems and to understand extensively the kinetics of a composite material, which does not follow a typical behavior of a salt hydrate nor of an adsorbent. Various prototype reactors and systems were developed by the scientific community to study the performances of sorption materials at macro-scale. Open and closed solid sorption systems have been analyzed and compared. Among the reviewed prototypes, mostly systems based on zeolites were able to achieve temperatures suitable for space heating or DHW production. For these systems, relatively high desorption temperatures were required, unachievable, for example, by conventional solar thermal collectors.

Dongdong Li (2018) studied on the development of a multi-temperature thermodynamically consistent model for salt lake brine systems. Under the comprehensive thermodynamic framework proposed in his previous work, the thermodynamic and phase equilibria properties of the sulfate binary systems (i.e., $Li_2SO_4 + H_2O$, $Na_2SO_4 + H_2O$, $K_2SO_4 + H_2O$, $MgSO_4 + H_2O$ and $CaSO_4 + H_2O$) were simulated using the Pitzer-Simonson Clegg (PSC) model. Various type of thermodynamic properties (i.e., water activity, osmotic coefficient, mean ionic activity coefficient, enthalpy of dilution and solution, relative apparent molar enthalpy, heat capacity of aqueous phase and solid phases) were collected and

fitted to the model equations. The thermodynamic properties of these systems can be well reproduced or predicted using the obtained model parameters.

Farzad Deyhimi (2009) studied the use of Pitzer, PSC as well as an extended PSC ion-interaction approaches for modelling the non-ideal behavior of the ternary HCl + water + 1- propanol systems. These modelling purposes were achieved based on the experimental potentiometric data of a galvanic cell containing a pH glass membrane and Ag/AgCl electrodes. The measurements were performed over the HCl electrolyte molality ranging from 0.01 up to 4.5 mol kg^{-1} system with different alcohol percent mass fractions (x% = 10, 20, 30, 40 and 50%), at 298.15 ± 0.05 K

Pitzer semi-empirical virial coefficient approach has been remarkably successful in modeling the thermodynamic properties of aqueous electrolyte solutions. Although this approach proved to be also a valuable method for correlation and prediction of thermodynamic properties of electrolytes in mixed solvent media, there is still only a limited number of reported studies concerning its application for modeling such systems. Pitzer and Simonson (PS) developed a newer model as well that is applicable over the entire concentration range for the investigation of mixtures containing ions of symmetrical charge type.
Both experimental potentiometric data along with the related model parameters associated with Pitzer, PSC, and an extended PSC approaches concerning the investigation of the ternary HCl + 1- PrOH + water electrolyte system, are for the first time reported in his work.

Edilson C. Tavares (1999) studied the solid-liquid equilibrium in aqueous multi-electrolyte systems using the quasiisothermic thermometric technique (QTT). The principle of the QTT is based on thermal effects associated with the phase transformations that occur in the system. In order to test the apparatus, salt solubility data at 298.15 K for the aqueous systems H_2O+NaCl+KCl, H_2O+NaCl+Na_2SO_4, H_2O+$NiCl_2$+$NiSO_4$ are presented. The data obtained for the

three systems are in good agreement with the literature, including solid phase boundaries due to hydration. This agreement indicates the accuracy of the proposed method.

The QTT has been properly tested for the measurement of salt solubilities and solid phase transitions. The apparatus is simple construction and can be operated with the aid of the computer interface, giving accurate data. The burette should be monitored via interface and computer. The QTT has been applied for the measurement of new salt solubility and solid phase transition data for the system $NiCl_2$+$NiSO_4$+H_2O at 298.15 K.

Huinan Wang (2020) Vapor–liquid equilibrium (VLE) data and modeling for LiBr + H_2O and LiBr + $CaCl_2$ + H_2O are reported in this paper. This work focuses on the experimental determination of the boiling point of LiBr + H_2O and LiBr + $CaCl_2$ + H2O solutions with vapor pressures between 6 and 101.3 kPa and the total molality of salt ranging from 0 to 21.05 $molkg^{-1}$. The procedures were carried out in a computer-controlled glass apparatus. The relationship between the boiling point and saturated vapor pressure is obtained, and Xu's model is used to correlate and predict the VLE. By correlation of the data (literature and experimental) for LiBr + H_2O and LiBr + $CaCl_2$ + H_2O, the parameters are obtained. e compared the results with the ElecNRTL model and Pitzer model. The parameters for the LiBr + H_2O, $CaCl_2$ + H_2O, and LiBr + $CaCl_2$ + H_2O systems can be successfully used to calculate and predict the VLE data

Christoph Rathgeber (2019) In this work, the modified BET equations are extended in order to calculate solubility phase diagrams of concentrated salt solutions with relatively high water activities within the range of undersaturation. Predicting solubility phase diagrams of mixtures of salts and water is of interest in various application fields, e.g. in the process of extracting salts or salt hydrates from natural salt brines to develop working fluids in absorption refrigeration systems, or to develop phase change materials for thermal energy storage . As an

example, BET parameters of NaCl are determined and applied to calculate solubility phase diagrams of NaCl + H_2O, NaCl + LiCl + H_2O, and NaCl + $CaCl_2$ + H_2O within the temperature range of around 250–500 K. In the ternary systems, the best agreement with solubility data from literature is obtained using constant BET parameters of NaCl and an additional temperature-dependent regular solution parameter to account for salt-salt interaction.

2.2 Various Models Available

Various Thermodynamic models are studied from literature.

1-Debye–Hückel equation

The Debye Hückel equation is a mathematical expression developed to explain certain properties of electrolyte solutions, or substances found in solutions in the form of charged particles (ions). The Debye Hückel equation accounts for the interactions between the different ions, which are the primary cause of differences between the properties of dilute electrolyte solutions and those of so-called ideal solutions.

The Debye-Hückel theory is based on three assumptions of how ions act in solution:

1. Electrolytes completely dissociate into ions in solution
2. Solutions of Electrolytes are very dilute, on the order of 0.01 M
3. Each ion is surrounded by ions of the opposite charge, on average

2- Davies equation

Davies equation is useful at ionic strengths up to 0.5M, making it a better choice than the Deybe-Huckel Model, It makes better calculation in concentrated solutions than Deybe-Huckel Model. This equation was originally published in 1938.The calculation gets deviated from experiment for electrolytes that disassociate into ions with higher charges

3 -Pitzer

Pitzer equations were first introduced by physical chemist Kenneth Pitzer. The parameters of Pitzer equations are linear combination of a parameters which differentiate amongst ions and solvent. The parameters are derived from various experimental data such as activity data and salt solubility. The equations are made of an extended Deybe-Huckel limiting law and a virial expansion. Pitzer equations are based on an ion interaction approach, where strong interactions are treated as ion pair formation but weaker interactions are treated as ion-ion interactions that contribute to the respective ions activity coefficients .The Pitzer equations are based on an extension of the Debye-Hückel equation using a virial equation approach, where the interactions between pairs and triplets of ions and molecules are described by empirical parameters. A Pitzer model is therefore dependent on a wealth of experimental data that underlie the database of Pitzer parameters. Pitzer modelling of the major components of seawater (seawater electrolyte) is well established, and is being applied to trace metals as the relevant experimental data become available.

4- B-E-T Method

BET method is also used for predicting phase change across a range of temperature and concentration. The main parameter used in BET modelling is r and ε. These parameters are temperature dependent. The number of binding sites on salt is represented by r and ε represents the difference between the molar enthalpy of adsorption of water on the salt and the molar enthalpy of liquefaction of water.

5- Pitzer Simonson Clegg

It is one of the most popular model for predicting behavior of mixed electrolytes. In the PSC model, the excess Gibbs energy is represented by summation of short-range and long-range interactions. The long-range forces contribution is represented by the extended DH expression and short-range interaction term is represented by Margules expansion which includes the parameters for the interaction of solvent -anion, solvent-cation, and the disassociation of all electrolyte.

2.3 Research gap

There is wide research gap in the Salt hydrates such as

1. Lack of experimental data at high temperature and pressure and validation,

2.Model accounting for salt hydrates at elevated temperature, pressure, and concentration

3. Accounting of unstable chemical reactions

4. Accounting of complex phase equilibria (vapor: liquid: solid).

CHAPTER 3

METHODOLOGY

3.1 Model 1

In this work, Gibbs free energy term is given by long range (Lr) electrostatic contributions b/w ions and short range (Sr) interaction b/w all species.

Using Pitzer`s form of the Debye- Huckle (PDH) function as the electrostatic contribution to the free energy. So

$$\frac{F^{Lr}}{RT} = -(v_w n_w + \upsilon v_s n_s)\frac{4A_\varphi I}{b} ln\left(1 + bI^{1/2}\right)$$

Where n_w, n_s = no. of moles of water, salt respectively

v_s, v_w = partial molar volume (m^3/mole) of salt, solvent respectively

b = the closest approach parameter

Total no. of ions per salt $\upsilon = \upsilon_M + \upsilon_X$

Debye Huckel type constant $A_\varphi = \frac{1}{3}\left[\frac{2\pi N_A}{V_S}\right]^{1/2}\left[\frac{e^2}{4\pi\varepsilon D_S KT}\right]^{3/2}$

Where Mw = molecular weight of solvent i.e., water in gram/mol,

N_A = Avogadro number,

K = Boltzmann constant, ε = permittivity of vacuum, e = electronic charge,

D_S = dielectric constant of water, V_S = the molar volume of water

I = the ionic strength $I = \sum C_i \frac{Z_i^2}{2}$ or $I = \frac{1}{2} C\upsilon|Z_+ Z_-|$

The expression for the short-range interaction contribution of aqueous salt solution is obtained from Flory- Huggins theory as given below,

$$\frac{F^{Sr}}{RT} = v_w n_W \, ln\, \varphi_w + \upsilon v_s n_s \, ln\, \varphi_s + \chi_{sw} v_w n_w \varphi_s$$

Where χ_{sw} = salt-water interaction parameter, which dependent on the salt concentration and temperature

$$\frac{F}{RT} = -(n_w + \nu n_s)\frac{4A_x I_x}{b}\ln\left(1 + bI_x^{1/2}\right) + n_w \ln\phi_w + \nu n_s \ln\phi_s + \chi_{sw}\, n_w \phi_s$$

where n_S and n_w represent the moles of salt hydrate and water in salt hydrate solution, respectively. r_S is the number of Kuhn segments in Salt hydrate chain. The term χ_{sw} is the generalized Flory-Huggins parameter and considered as the function of the volume fraction of the salt hydrate, ϕ_S, and temperature, T.

$$\chi_{sw}(T, \phi_S) = \sum_{i=0}^{n} b_i(T)\, \phi_S^i$$

$b_i(T)$ is temperature dependent coefficient and as expressed as:

$$b_i(T) = b_{i\alpha} + b_{i\beta}\left(\frac{1}{T} - \frac{1}{T_r}\right) + b_{i\gamma}\, ln\left({}^{T}/_{T_r}\right)$$

$b_{i\alpha}, b_{i\beta}$ and $b_{i\gamma}$ are constants

$b_i(T)$ is temperature dependent coefficient are calculated using non linear regression method

Derivative of Equation (1) w.r.t. moles of water and salt gives us chemical potential of water and salt hydrate respectively.

$$\frac{\mu_w - \mu_w^0}{RT} = \left(\delta \frac{F}{\frac{RT}{\delta n_w}}\right)_{n_s}$$

$$= \left(\mathrm{I_x}\ln\left(1 + bI_x^{1/2}\right)\right)\left[-\frac{\nu n_s}{n_w}\right] - \frac{(n_w + \nu n_s)}{2\left(1 + bI_x^{1/2}\right)}\frac{I_x^{-1/2}}{n_w} + \ln\phi_w$$

$$+ \phi_s\left(1 - \frac{v_w}{v_s}\right) - \chi_{sw}\phi_s^2 - \frac{\delta\chi_{sw}}{\delta\phi_s}\phi_s^2(1 - \phi_s)$$

$$\frac{\mu_s - \mu_s^0}{RT} = \left(\delta \frac{F}{\frac{RT}{\delta n_s}}\right)_{n_s}$$

$$= I_x\ln\left(1 + bI_x^{1/2}\right)\left(2 + \frac{n_w}{n_s}\right) + \left(\frac{n_w}{n_s} + \nu\right)\left(\frac{1}{\left(1 + bI_x^{1/2}\right)}\, b\frac{1}{2}I_x^{\frac{3}{2}}\right)$$

$$+ \nu\,[\ln\phi_s + \left(1 - \frac{v_S}{v_w}\right)\phi_w + \frac{v_s}{v_w}\,\chi_{sw}(1 - \phi_s)^2$$

$$+ \frac{v_s}{v_w}\phi_s(1 - \phi_s)^2\,\frac{\delta\chi_{sw}}{\delta\phi_s}$$

The condition for the phase equilibrium between two separate phases (Phase-1 and Phase-2) are given by

$\mu_w^\alpha = \mu_w^\beta$

And $\mu_S^\alpha = \mu_S^\beta$

By solving equation simultaneously, phase diagram can be obtained.

$$\frac{\ln(1 - \phi_s^\alpha)}{\ln(1 - \phi_s^\beta)} + \left(\phi_s^\alpha - \phi_s^\beta\right)\left(1 - \frac{v_w}{v_s}\right)$$

$$- \left[\chi_{sw}(T, \phi_s^\alpha)\,\phi_s^{2\alpha} + \frac{\delta\chi_{sw}(T, \phi_s^\alpha)}{\delta\phi_s^\beta}\phi_s^{2\alpha}(1 - \phi_s^\alpha)\right]$$

$$- \left[\chi_{sw}\left(T, \phi_s^\beta\right)\phi_s^{2\beta} + \frac{\delta\chi_{sw}\left(T, \phi_s^\beta\right)}{\delta\phi_s^\beta}\phi_s^{2\beta}\left(1 - \phi_s^\beta\right)\right] = 0$$

$$v\left[\ln\frac{\phi_s^\alpha}{\phi_s^\beta}+\left(1-\frac{v_S}{v_w}\right)\left(2-\phi_s^\alpha-\phi_s^\beta\right)\right]$$
$$+\left[\frac{v_s}{v_w}\,\chi_{sw}\,(T,\phi_s^\alpha)(1-\phi_s^\alpha)^2+\frac{v_s}{v_w}\phi_s^\alpha(1-\phi_s^\alpha)^2\,\frac{\delta\chi_{sw}(T,\phi_s^\alpha)}{\delta\phi_s^\alpha}\right]$$
$$+\left[\frac{v_s}{v_w}\,\chi_{sw}\left(T,\phi_s^\beta\right)\left(1-\phi_s^\beta\right)^2+\frac{v_s}{v_w}\phi_s^\beta\left(1-\phi_s^\beta\right)^2\,\frac{\delta\chi_{sw}\left(T,\phi_s^\beta\right)}{\delta\phi_s^\beta}\right]$$
$$=0$$

The critical point is given by the following conditions :

$$\frac{\delta^2\left(\frac{F}{RT}\right)}{\delta\phi_s^2}=\frac{\delta^2\left(\frac{F}{RT}\right)}{\delta\phi_s^3}$$

$$\frac{\delta^2\left(\frac{F}{RT}\right)}{\delta\phi_s^2} = \left(\left(\left(-\frac{\frac{v_s}{v_w}vn_s}{\phi_s^2} + v\frac{n_s}{\phi_s(1-\phi_s)}\right)\right) I_x \frac{1}{\phi_s(1-\phi_s)}\left(\ln\left(1+bI_x^{\frac{1}{2}}\right) + \frac{1}{2}\, I_x^{\frac{1}{2}}\, \frac{1}{1+bI_x^{\frac{1}{2}}}\right)\right)$$

$$+ (n_w + vn_s)\frac{I_x}{\left(\phi_s(1-\phi_s)\right)^2}\left(\ln\left(1+bI_x^{\frac{1}{2}}\right) + \frac{1}{2}\, I_x^{\frac{1}{2}}\, \frac{1}{1+bI_x^{\frac{1}{2}}}\right)$$

$$+ (n_w + vn_s)\, I_x \frac{1}{\phi_s(1-\phi_s)}\frac{b}{1+bI_x^{\frac{1}{2}}}\frac{1}{4}\left(2I_x^{\frac{1}{2}} + \frac{I_x^{\frac{-1}{2}}}{b} - 1\right)$$

$$+\left(\left(-\frac{v_s}{v_w}v\left(\frac{n_s}{\phi_s^3}\frac{-1+2\phi_s}{1-\phi_s}\right) + \left(\frac{n_s}{\phi_s^2(1-\phi_s)^2} + n_s\frac{2\phi_s-1}{\phi_s^2(1-\phi_s)^2}\right)\right) I_x \ln\left(1+bI_x^{\frac{1}{2}}\right)\right)$$

$$+\left(\left(-\frac{\frac{v_s}{v_w}vn_s}{\phi_s^2} + \frac{n_s}{\phi_s(1-\phi_s)}\right)\left(\frac{I_x}{\phi_s(1-\phi_s)}\right)\ln\left(1+bI_x^{\frac{1}{2}}\right)\right)$$

$$+\left(\left(-\frac{\frac{v_s}{v_w}vn_s}{\phi_s^2} + \frac{n_s}{\phi_s(1-\phi_s)}\right) I_x^{\frac{3}{2}}\frac{1}{\left(1+bI_x^{\frac{1}{2}}\right)}\, b\frac{1}{2}\frac{1}{\phi_s(1-\phi_s)}\right)$$

$$+ -\frac{v_s}{v_w}v\left[\frac{n_s}{\varphi_s(1-\varphi_s)}\,\frac{1}{\phi_s^3(1-\phi_s)}\,ln(1-\phi_s)\right) + n_s\left(\frac{4\phi_s-3}{\phi_s^4(1-\phi_s)^4}\right) ln(1-\phi_s)$$

$$+ \quad n_s\frac{-1}{\phi_s^3(1-\phi_s)^2}\Big] + (-2)\left(\left(\frac{n_s}{\varphi_s^4(1-\varphi_s)}\ln(1-\phi_s)\right) + n_s(-3)\,\phi_s^{-4}\ln(1-\phi_s)\right)$$

$$+ n_s\phi_s^{-3}\frac{-1}{\phi_s-1}) + \; n_s\,\frac{(-1)}{\phi_s^3(1-\phi_s)^2} + n_s(-1)\,\frac{3\phi_s-2}{(\phi_s-1)^2\phi_s^3}\Big] - \Big[-\frac{\frac{v_s}{v_w}vn_s}{\phi_s^2}\,\frac{1}{(1-\phi_s)^2}$$

$$+ n_w\frac{2}{(1-\phi_s)^3} + \left(\frac{v_s}{v_w}v\right)\left(-\frac{\frac{v_s}{v_w}vn_s}{\phi_s^2}\, n_s\,\frac{1}{\phi_s^2} + n_w\,\frac{n_s}{\varphi_s(1-\varphi_s)}\,\frac{1}{\phi_s^2} + n_w n_s(2)\phi_s^{-3}\right)$$

$$+ -\frac{v_s}{v_w}v\left[\frac{n_s}{\varphi_s(1-\varphi_s)}\,\frac{1}{\phi_s^3(1-\phi_s)}\,ln(1-\phi_s)\right) + n_s\left(\frac{4\phi_s-3}{\phi_s^4(1-\phi_s)^4}\right) ln(1-\phi_s)$$

$$+ \quad n_s\frac{-1}{\phi_s^3(1-\phi_s)^2}\Big] + (-2)\left(\left(\frac{n_s}{\varphi_s^4(1-\varphi_s)}\ln(1-\phi_s)\right) + n_s(-3)\,\phi_s^{-4}\ln(1-\phi_s)\right)$$

$$+ n_s\phi_s^{-3}\frac{-1}{\phi_s-1}) + \; n_s\,\frac{(-1)}{\phi_s^3(1-\phi_s)^2} + n_s(-1)\,\frac{3\phi_s-2}{(\phi_s-1)^2\phi_s^3}\Big] - \Big[-\frac{\frac{v_s}{v_w}vn_s}{\phi_s^2}\,\frac{1}{(1-\phi_s)^2}$$

$$+ n_w\frac{2}{(1-\phi_s)^3} + \left(\frac{v_s}{v_w}v\right)\left(-\frac{\frac{v_s}{v_w}vn_s}{\phi_s^2}\, n_s\,\frac{1}{\phi_s^2} + n_w\,\frac{n_s}{\varphi_s(1-\varphi_s)}\,\frac{1}{\phi_s^2} + n_w n_s(2)\phi_s^{-3}\right)\Big]$$

$$\frac{\delta^3\left(\frac{F}{RT}\right)}{\delta\phi_s^3}=\left(\frac{1}{1+bI_x^{\frac{1}{2}}}\frac{1}{2}\left(\frac{I_x^{\frac{1}{2}}}{\phi_s(1-\phi_s)}+\frac{1}{2}I_x^{\frac{-1}{2}}-\frac{1}{4}\frac{1}{1+bI_x^{\frac{1}{2}}}I_x\frac{1}{\phi_s(1-\phi_s)}\right)\right)I_x\frac{1}{\phi_s(1-\phi_s)}\left(-\frac{\frac{v_s}{v_w}\nu n_s}{\phi_s^2}+\nu\frac{n_s}{\phi_s(1-\phi_s)}+\right.$$
$$\left.(n_w+\nu n_s)\frac{I_x}{\phi_s(1-\phi_s)}\right)+\left(\ln\left(1+bI_x^{\frac{1}{2}}\right)+\frac{1}{2}I_x^{\frac{1}{2}}\frac{1}{1+bI_x^{\frac{1}{2}}}\right)\left(\frac{I_x}{\phi_s(1-\phi_s)}\right)\frac{1}{\phi_s(1-\phi_s)}\left(-\frac{\frac{v_s}{v_w}\nu n_s}{\phi_s^2}+\nu\frac{n_s}{\phi_s(1-\phi_s)}+\right.$$
$$\left.(n_w+\nu n_s)\frac{I_x}{\phi_s(1-\phi_s)}\right)+\left(\ln\left(1+bI_x^{\frac{1}{2}}\right)+\frac{1}{2}I_x^{\frac{1}{2}}\frac{1}{1+bI_x^{\frac{1}{2}}}\right)I_x\left(-\frac{2\phi_s-1}{(\phi_s(1-\phi_s))^2}\right)\left(-\frac{\frac{v_s}{v_w}\nu n_s}{\phi_s^2}+\nu\frac{n_s}{\phi_s(1-\phi_s)}+\right.$$
$$\left.(n_w+\nu n_s)\frac{I_x}{\phi_s(1-\phi_s)}\right)+\left(\ln\left(1+bI_x^{\frac{1}{2}}\right)+\frac{1}{2}I_x^{\frac{1}{2}}\frac{1}{1+bI_x^{\frac{1}{2}}}\right)I_x\frac{1}{\phi_s(1-\phi_s)}\left(\left(-\frac{v_s}{v_w}\nu\left(\frac{n_s}{\phi_s(1-\phi_s)}\phi_s^{-2}+\right.\right.\right.$$
$$\left.\left.\left.n_s(-2\phi_s^{-1})\right)+\nu\left(\left(\frac{n_s}{\phi_s(1-\phi_s)}\right)\frac{1}{\phi_s(1-\phi_s)}+n_s\left(-\frac{2\phi_s-1}{(\phi_s(1-\phi_s))^2}\right)+\left(-\frac{\frac{v_s}{v_w}\nu n_s}{\phi_s^2}+\nu\frac{n_s}{\phi_s(1-\phi_s)}\right)\frac{I_x}{\phi_s(1-\phi_s)}+\right.\right.\right.$$
$$\left.\left.\left.(n_w+\nu n_s)\left(\frac{I_x}{\phi_s(1-\phi_s)}\right)\frac{1}{\phi_s(1-\phi_s)}\right)+(n_w+\nu n_s)I_x\left(-\frac{2\phi_s-1}{(\phi_s(1-\phi_s))^2}\right)\right)+\frac{1}{4}b\left(\left(-\left(1+\right.\right.\right.\right.$$
$$\left.\left.\left.\left.bI_x^{\frac{1}{2}}\right)^{-2}bI_x^{\frac{-1}{2}}\right)(n_w+\nu n_s)\left(2I_x^{\frac{3}{2}}+\frac{I_x^{\frac{1}{2}}}{b}-1\right)+\frac{1}{1+bI_x^{\frac{1}{2}}}\left(\left(-\frac{\frac{v_s}{v_w}\nu n_s}{\phi_s^2}+\nu\frac{n_s}{\phi_s(1-\phi_s)}\right)\right)\left(2I_x^{\frac{3}{2}}+\frac{I_x^{\frac{1}{2}}}{b}-1\right)\right)\right)+$$
$$\frac{1}{1+bI_x^{\frac{1}{2}}}(n_w+\nu n_s)\left(\left(3I_x^{\frac{1}{2}}+\frac{1}{2}\frac{1}{b}I_x^{\frac{-1}{2}}\right)\right)\left(\left(\left(\frac{n_s}{\phi_s(1-\phi_s)}\right)\left(-\frac{v_s}{v_w}v\left(\frac{-1+2\phi_s}{(1-\phi_s)\phi_s^3}\right)+\left(\frac{2}{\phi_s(1-\phi_s)^2}\right)\right)I_x\ln\left(1+\right.\right.\right.\right.$$
$$\left.\left.\left.\left.bI_x^{\frac{1}{2}}\right)\right)\right)\left(\left(\left(n_s\left(\frac{\delta}{\delta\phi_s}\left(-\frac{v_s}{v_w}v\left(\frac{6\phi_s^2-8\phi_s+3}{\phi_s^4(1-\phi_s)^2}\right)+\left(2\frac{3\phi_s+1}{\phi_s^2(\phi_s-1)^3}\right)\right)\right)I_x\ln\left(1+\right.\right.\right.\right.$$
$$\left.\left.\left.\left.bI_x^{\frac{1}{2}}\right)\right)\right)\left(\left(n_s\left(-\frac{v_s}{v_w}v\left(\frac{-1+2\phi_s}{(1-\phi_s)\phi_s^3}\right)+\left(\frac{2}{\phi_s(1-\phi_s)^2}\right)\right)\left(\frac{\delta}{\delta\phi_s}I_x\right)\ln\left(1+\right.\right.\right.\right.$$
$$\left.\left.\left.\left.bI_x^{\frac{1}{2}}\right)\right)\right)\left(\left(n_s\left(-\frac{v_s}{v_w}v\left(\frac{-1+2\phi_s}{(1-\phi_s)\phi_s^3}\right)+\left(\frac{2}{\phi_s(1-\phi_s)^2}\right)\right)I_x\left(I_x^{\frac{3}{2}}\frac{1}{\left(1+bI_x^{\frac{1}{2}}\right)}b\frac{1}{2}\right)\right)\right)+$$
$$\left(\left(\left(-\frac{v_s}{v_w}v\left(\frac{n_s}{\phi_s^3}\frac{-1+2\phi_s}{1-\phi_s}\right)+\left(\frac{n_s}{\phi_s^2(1-\phi_s)^2}+n_s\frac{2\phi_s-1}{\phi_s^2(1-\phi_s)^2}\right)\right)\left(\frac{I_x}{n_s}\right)\ln\left(1+bI_x^{\frac{1}{2}}\right)\right)\right)+$$
$$\left(\left(\left(-\frac{v_s}{v_w}v\left(\frac{n_s}{\phi_s^3}\frac{-1+2\phi_s}{1-\phi_s}\right)+\left(\frac{n_s}{\phi_s^2(1-\phi_s)^2}+n_s\frac{2\phi_s-1}{\phi_s^2(1-\phi_s)^2}\right)\right)I_x\left(I_x^{\frac{3}{2}}\frac{1}{\left(1+bI_x^{\frac{1}{2}}\right)}b\frac{1}{2}\right)\right)\right)+$$
$$\left(\frac{n_s}{\phi_s(1-\phi_s)}\right)\left(-\frac{\frac{v_s}{v_w}v}{\phi_s^2}+\frac{1}{\phi_s(1-\phi_s)}\right)\left(\frac{1}{\phi_s(1-\phi_s)}\right)I_x\ln\left(1+bI_x^{\frac{1}{2}}\right)+n_s\left(\frac{\delta}{\delta\phi_s}\left(2\frac{\frac{v_s}{v_w}v}{\phi_s}+\right.\right.$$
$$\left.\left.\frac{1}{\phi_s(1-\phi_s)}\right)\right)\left(\frac{1}{\phi_s(1-\phi_s)}\right)I_x\ln\left(1+bI_x^{\frac{1}{2}}\right)+n_s\left(-\frac{\frac{v_s}{v_w}v}{\phi_s^2}+\frac{1}{\phi_s(1-\phi_s)}\right)\left(\frac{2\phi_s-1}{\phi_s^2(1-\phi_s)^2}\right)I_x\ln\left(1+bI_x^{\frac{1}{2}}\right)+$$
$$n_s\left(-\frac{\frac{v_s}{v_w}v}{\phi_s^2}+\frac{1}{\phi_s(1-\phi_s)}\right)\left(\frac{1}{\phi_s(1-\phi_s)}\right)\left(\frac{I_x}{n_s}\right)\ln\left(1+bI_x^{\frac{1}{2}}\right)+n_s\left(-\frac{\frac{v_s}{v_w}v}{\phi_s^2}+\right.$$

$$\frac{1}{\phi_s(1-\phi_s)}\Big)\Big(\frac{1}{\phi_s(1-\phi_s)}\Big)I_x^{\frac{5}{2}}\frac{1}{\left(1+bI_x^{\frac{1}{2}}\right)}\,b\frac{1}{2}+b\frac{1}{2}\,[\left(\left(\frac{n_s}{\phi_s(1-\phi_s)}\right)\left(-\frac{\frac{v_s}{v_w}v}{\phi_s^2}+\frac{1}{\phi_s(1-\phi_s)}\right)I_x^{\frac{3}{2}}\frac{1}{\left(1+bI_x^{\frac{1}{2}}\right)}\frac{1}{\phi_s(1-\phi_s)}\right)+$$

$$\left(n_S\left(\frac{\delta}{\delta\phi_s}\left(2\frac{\frac{v_s}{v_w}v}{\phi_s}+\frac{2\phi_s-1}{(\phi_s-1)^2\phi_s^2}\right)\right)I_x^{\frac{3}{2}}\frac{1}{\left(1+bI_x^{\frac{1}{2}}\right)}\frac{1}{\phi_s(1-\phi_s)}\right)+\left(\left(-\frac{\frac{v_s}{v_w}v}{\phi_s^2}+\right.\right.$$

$$\left.\frac{1}{\phi_s(1-\phi_s)}\Big)\Big(\frac{3}{2}\Big)\frac{I_x^{\frac{3}{2}}}{n_s}\frac{1}{\left(1+bI_x^{\frac{1}{2}}\right)}\frac{1}{\phi_s(1-\phi_s)}\right)+\left(n_S\left(-\frac{\frac{v_s}{v_w}v}{\phi_s^2}+\frac{1}{\phi_s(1-\phi_s)}\right)I_x^2\left(\frac{1}{2}\frac{b}{\left(1+bI_x^{\frac{1}{2}}\right)^2}\right)\frac{1}{\phi_s(1-\phi_s)}\right)+$$

$$n_S\left(-\frac{\frac{v_s}{v_w}v}{\phi_s^2}+\frac{1}{\phi_s(1-\phi_s)}\right)I_x^{\frac{3}{2}}\frac{1}{\left(1+bI_x^{\frac{1}{2}}\right)}\left(\frac{2\phi_s-1}{(\phi_s-1)^2\phi_s^2}\right)++v[n_s\;\ln\phi_s\frac{1}{(\phi_s(1-\phi_s))^3}+n_s\;\frac{1}{\phi_s^3(1-\phi_s)^2}+$$

$$n_s\ln\phi_s\left(\frac{-3\phi_s+1}{(\phi_s-1)^3\phi_s^2}\right)+n_s\;\frac{1}{\phi_s^3(1-\phi_s)^2}+n_s\left(\frac{-3\phi_s+2}{(\phi_s-1)^2\phi_s^3}\right)+\frac{n_s}{\phi_s^3(1-\phi_s)^3}\ln\phi_s\;1-2\phi_s+n_s\;\left(\frac{1}{\phi_s^3}\right)\;2\frac{2\phi_s-1}{(\phi_s-1)^2}+$$

$$n_s\;\ln\phi_s(-2)(\frac{3\phi_s^2-3\phi_s+1}{(\phi_s-1)^3\phi_s^3})+n_s\;\frac{(-1)}{\phi_s^5(1-\phi_s)^2}+n_s\left(\frac{5\phi_s-4}{(\phi_s-1)^2\phi_s^5}\right)+\frac{\delta}{\delta\phi_s}\;(\left(\frac{\delta^2\chi_{sw}}{\delta\varphi_s^2}\right)(n_w)(\varphi_s)\;+$$

$$\left(\frac{\delta\chi_{sw}}{\delta\varphi_s}\right)\left(-\frac{\frac{v_s}{v_w}vn_s}{\phi_s}\right)+\left(\frac{\delta\chi_{sw}}{\delta\varphi_s}\right)(n_w)-\frac{v_s}{v_w}v\left[\frac{\delta\chi_{sw}}{\delta\varphi_s}\left(\frac{n_S}{\phi_s}+n_w\right)+\chi_{sw}\left(n_s\frac{1}{\phi_s^2(1-\phi_s)}+\;n_s\phi_s^{-2}+n_w+\right.\right.$$

$$\left.\left.\left(-\frac{\frac{v_s}{v_w}vn_s}{\phi_s^2}\right)\right)\right]$$

3.2 Model 2

We assume that the molar gibbs energy of mixing contains an electrostatic contribution given by a Deybe Huckel-type function and a contribution from extended Flory-Huggins theory ,as follows:

$$\frac{\Delta G}{RT} = \frac{\Delta G^{DH}}{RT} + \frac{\Delta G^{FH}}{RT}$$

Where superscripts DH and FH denote Deybe Huckel and Flory Huggins Contribution, respectively

Pizer's form of the Deybe-Huckel type function as the electrostatic contribution to the molar Gibbs energy of mixing is given by

$$\frac{\Delta G^{DH}}{RT} = \phi_1 (\frac{W}{1000}) \left[-A_\Phi \left(\frac{4I}{b} \right) \ln \left(1 + bI^{\frac{1}{2}} \right) \right]$$

Where $I = \frac{1}{2} \left[\frac{\phi_2 \left(\frac{1000}{W} \right)}{\phi_1} \right] |z_m z_x|$

$$The\ values\ for\ A_\Phi = 0.392\ and\ b = 1.2\ at\ 25^0 C$$

The electrostatic contribution does not contain adjustable parameters.

The Flory-Huggins contribution to the molar Gibbs energy of mixing is given by the following

$$\frac{\Delta G^{FH}}{RT} = \phi_1 \ln \phi_1 + \phi_2 \ln \phi_2 + g_{12}(\phi_2)\phi_1\phi_2$$

Where the first two terms and the last term on the right hand side of equation represent, respectively, the configurational entropy of mixing and the residual free-energy, mostly enthalphic ,interaction between water and salt ion .

g_{12} refers the interaction between water and ion. It is interaction parameter.

For a binary salt water system Deybe Huckel and Flory Huggins contribution are combined to give the molar Gibbs energy of mixing given by

$$\frac{F}{RT} = \phi_1\left(\frac{W}{1000}\right)\left[-A_\Phi\left(\frac{4I}{b}\right)\ln\left(1+bI^{\frac{1}{2}}\right)\right] + \phi_1\ln\phi_1 + \phi_2\ln\phi_2 + g_{12}(\phi_2)\phi_1\phi_2$$

$$g_{12}(\phi_2) = \sum c_k\phi_2^{k-1}$$

The condition for the phase equilibrium between two separate phases (Phase-1 and Phase-2) are given by

$$\ln a_w = \frac{\mu_w - \mu_w^0}{RT} = \left(\delta\frac{\frac{F}{RT}}{\delta n_w}\right)_{n_s} = \frac{2\ A_\Phi I^{\frac{3}{2}}}{1+bI^{\frac{1}{2}}} + \ln\phi_1 + (\phi_1^2 g_{12} - \phi_1\phi_2 g'_{12})$$

$$\ln\beta_w = \frac{\mu_s - \mu_s^0}{RT} = \left(\delta\frac{\frac{F}{RT}}{\delta n_s}\right)_{n_s} = c\left[\left(\left(\frac{v}{n_w}(1-\phi_2)\right)I\ \ln\left(1+bI^{\frac{1}{2}}\right)\right) + (1-\phi_2)\left(c_1\frac{v}{n_w}\frac{1}{1-\phi_2}\right)\ln\left(1+bI^{\frac{1}{2}}\right)\right.$$
$$\left. +\ I^{\frac{1}{2}}\frac{1}{1+bI^{\frac{1}{2}}}b\frac{1}{2}\ \left(c_1\frac{v}{n_w}\right)\right] + -\frac{v}{n_w}(1-\phi_2)\left(\ln\left(\frac{\phi_2}{1-\phi_2}\right)+2\right) + \frac{\delta g_{12}(\phi_2)}{\delta\phi_2}\frac{v}{n_w}(1-\phi_2)\phi_2$$
$$+ g_{12}(\phi_2)\left(\frac{\delta}{\delta n_p}\phi_1\right)\phi_2 + g_{12}(\phi_2)\phi_1\left(\frac{\delta}{\delta n_p}\phi_2\right)$$
$$c = \left(\left(\frac{W}{1000}\right) - A_\Phi\left(\frac{4}{b}\right)\right)\ ;\ c_1 = \frac{1}{2}\left(\frac{1000}{W}\right)|z_m z_x|$$

$\mu_w^\alpha = \mu_w^\beta$

And $\mu_S^\alpha = \mu_S^\beta$

By solving equation and simultaneously, phase diagram can be obtained.

Phase Diagram equations

$$(1-\phi_2^\alpha)\left(\ln\left(\frac{\phi_2^\alpha}{1-\phi_2^\alpha}\right)+2\right) - (1-\phi_2^\beta)\left(\ln\left(\frac{\phi_2^\beta}{1-\phi_2^\beta}\right)+2\right)$$
$$+\left(\frac{\delta g_{12}(\phi_2^\alpha)}{\delta\phi_2^\alpha}(1-\phi_2^\alpha)^2\phi_2^\alpha + g_{12}(\phi_2^\alpha)\left(\left(-3\phi_2^\alpha + 2{\phi_2^\alpha}^2 + 1\right)\right)\right)$$
$$-\left(\frac{\delta g_{12}(\phi_2^\beta)}{\delta\phi_2^\beta}\left(1-\phi_2^\beta\right)^2\phi_2^\beta + g_{12}(\phi_2^\beta)\left(\left(-3\phi_2^\beta + 2{\phi_2^\beta}^2 + 1\right)\right)\right)$$
$$+\left[\left(((1-\phi_2^\alpha))I^\alpha\ \ln\left(1+bI^{\alpha\frac{1}{2}}\right)\right) + (c_1)\ \ln\left(1+bI^{\alpha\frac{1}{2}}\right) + I^{\alpha\frac{1}{2}}\frac{1}{1+bI^{\alpha\frac{1}{2}}}b\frac{1}{2}\ (c_1)\right]$$
$$-\left[\left(\left(\left(1-\phi_2^\beta\right)\right)I^\beta\ \ln\left(1+bI^{\beta\frac{1}{2}}\right)\right) + (c_1)\ \ln\left(1+bI^{\beta\frac{1}{2}}\right)\right.$$
$$\left. +\ I^{\beta\frac{1}{2}}\frac{1}{1+bI^{\beta\frac{1}{2}}}b\frac{1}{2}\ (c_1)\right]$$

$$\ln\left(\frac{1-\phi_2^{\alpha}}{1-\phi_2^{\beta}}\right)+\left[\left(\phi_2^{\alpha}\ \ g_{12}(\phi_2^{\alpha})-\left(\phi_2^{\alpha 2}-\ \phi_2^{\alpha 3}\right)\frac{\delta g_{12}(\phi_2^{\alpha})}{\delta\phi_2^{\alpha}}\right)\right.$$
$$\left.-\left(\phi_2^{\beta}\ \ g_{12}(\phi_2^{\beta})-\left(\phi_2^{\beta^2}-\ \phi_2^{\beta^3}\right)\frac{\delta g_{12}(\phi_2^{\beta})}{\delta\phi_2^{\beta}}\right)\right]+\left[\frac{I^{\alpha^{\frac{3}{2}}}}{1+bI^{\alpha^{\frac{1}{2}}}}-\frac{I^{\beta^{\frac{3}{2}}}}{1+bI^{\beta^{\frac{1}{2}}}}\right]$$

Critical Point equations

$$\frac{\delta^2(\frac{F}{RT})}{\delta\phi_2^2}=\frac{\delta^3(\frac{F}{RT})}{\delta\phi_2^3}$$

$$\frac{\delta^2(\frac{F}{RT})}{\delta\phi_2^2}=-I\ln\left(1+bI^{\frac{1}{2}}\right)+c_1\ln\left(1+bI^{\frac{1}{2}}\right)+I^{\frac{1}{2}}\frac{1}{1+bI^{\frac{1}{2}}}\frac{1}{2}\frac{c_1}{1-\phi_2}+\ln\frac{\phi_2}{1-\phi_2}+\ \frac{\delta g_{12}(\phi_2)}{\delta\phi_2}\ \ (\phi_2-\phi_2^2)$$
$$+\ g_{12}(\phi_2)\ (1-2\phi_2)$$

$$\frac{\delta^3(\frac{F}{RT})}{\delta\phi_2^3}=\frac{1}{1-\phi_2}+\frac{1}{\phi_2}+\frac{\delta^2 g_{12}(\phi_2)}{\delta\phi_2^2}\ (\phi_2-\phi_2^2)+\frac{\delta g_{12}(\phi_2)}{\delta\phi_2}\ 2\ (1-2\phi_2)-\ 2\ g_{12}(\phi_2)$$
$$+\frac{c_1}{(1-\phi_2^2)}\left(-\ln\left(1+bI^{\frac{1}{2}}\right)-\frac{I}{1+bI^{\frac{1}{2}}}\right)+c_1\ \frac{I}{1+bI^{\frac{1}{2}}}\ b\frac{1}{2}\ I^{\frac{-1}{2}}\frac{c1}{(1-\phi_2)^2}$$

CHAPTER 4

RESULTS AND DISCUSSION

4.1 Parity Plot

1 -NaCl

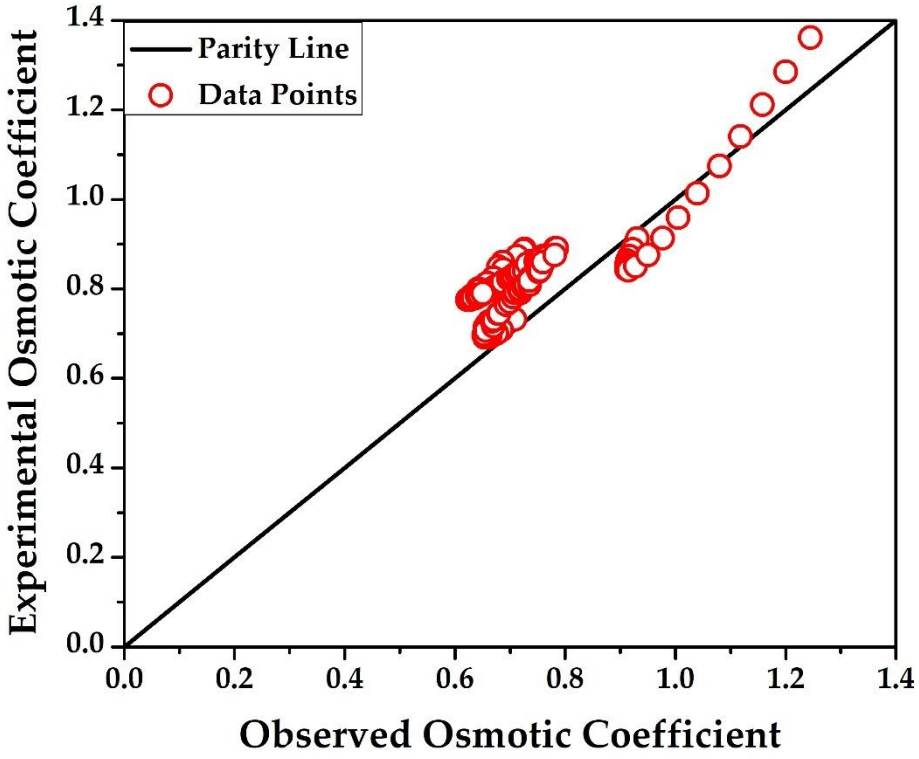

2-LiCl

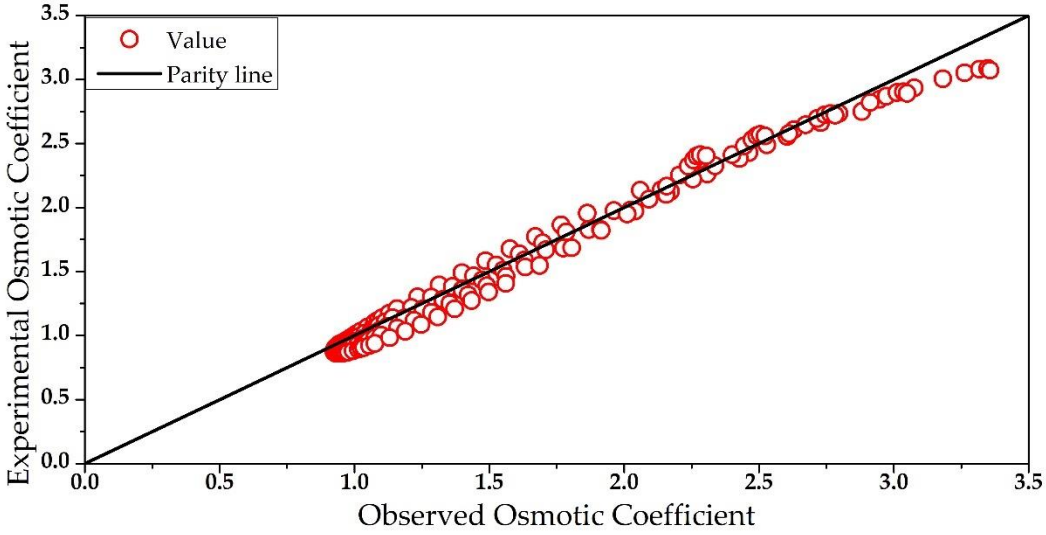

3-$CaCl_2$

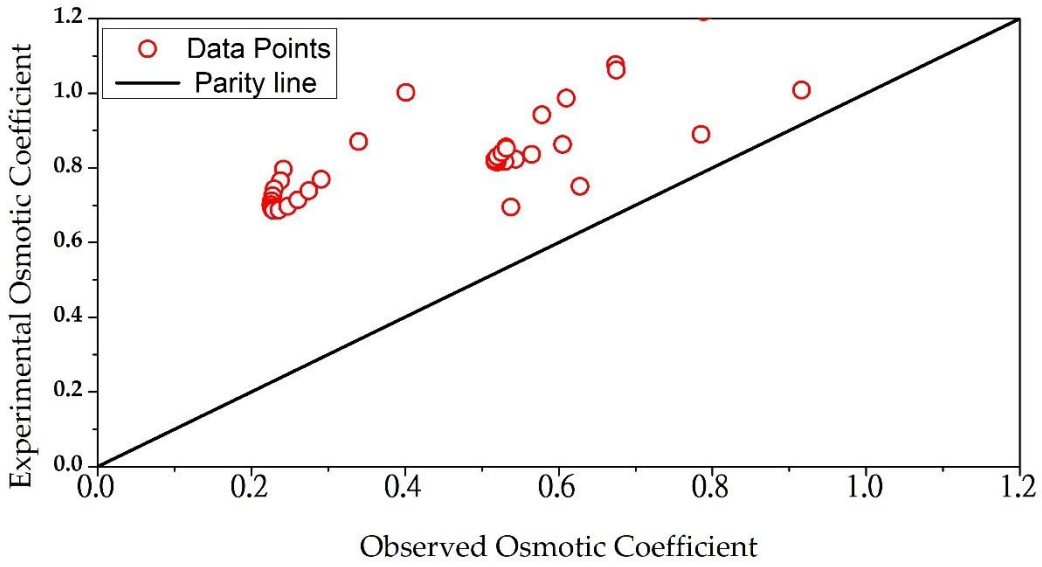

4-$MgSO_4$

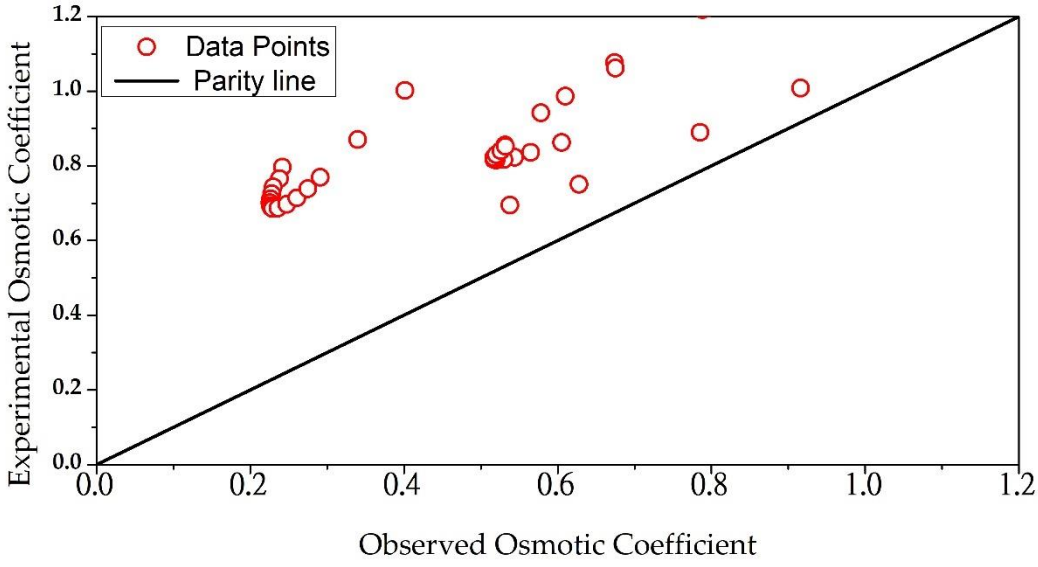

5-Li_2SO_4

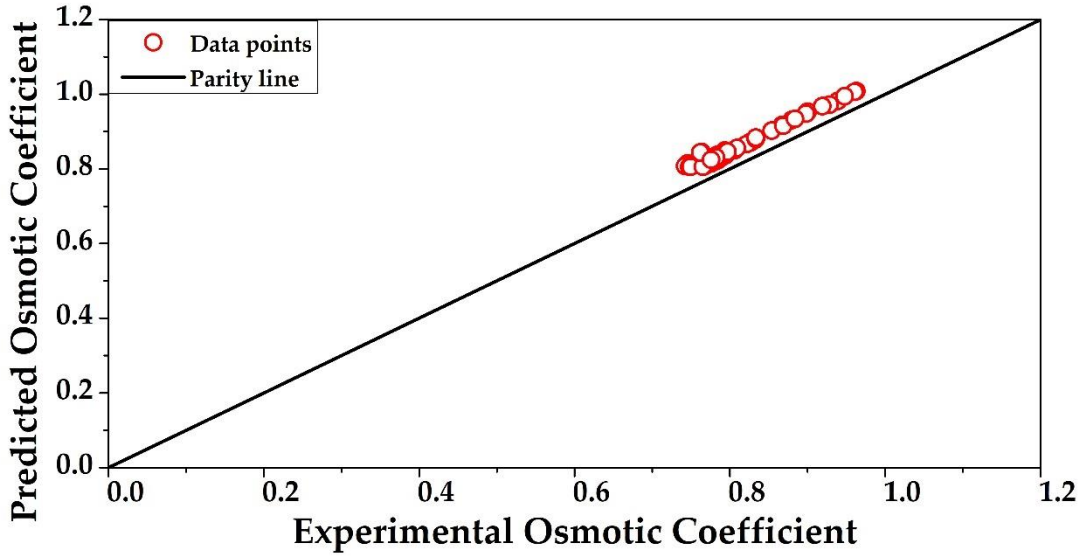
Data points
Parity line
Predicted Osmotic Coefficient
Experimental Osmotic Coefficient
0.0
0.2
0.4
0.6
0.8
1.0
1.2

4.2 Critical Point

Salt	ϕ_s	Temperature	Literature Critical Temperature	Deviation	Reference
NaCl	0.1506340	214.799	253.153	17.85%	[11]
LiCl	0.15237	200.0489	193.31	3.35%	[12]
$CaCl_2$	0.29971	243.15	223.388	8.127%	[13]
$MgSO_4$	0.104073	287.972	291.19	1.117%	[14]
Li_2SO_4	0.152345	260.824	251.515	3.569%	[15]

4.3 Regarding Parameters

a	*0*	*0*	*51.9789*	*$4.5x10^{-7}$*	*$3.8x10^{-8}$*
b	*1.274642*	*1.27485*	*0*	*1.27012*	*1.27515*
c	*15.92609*	*11.6397*	*0*	*53.8784*	*5.98346*
d	*93.45038*	*75.575*	*139.892*	*305.534*	*39.8211*
e	*0.534174*	*0.53407*	*7.41714*	*0.53537*	*0.53411*
f	*0*	*0*	*0*	*0*	*0*
g	*60.15876*	*44.7589*	*0*	*194.162*	*36.7534*
h	*0.987123*	*0.99022*	*3.14758*	*0.98586*	*0.9871*
i	*0*	*0*	*0*	*0.42987*	*0*
j	*1.035697*	*1.03633*	*0*	*1.00217*	*1.03091*
k	*1.982129*	*1.82918*	*0*	*2.78937*	*1.98314*
l	*9.659121*	*7.31275*	*0*	*34.3719*	*0.00967*
m	*3.037581*	*3.05209*	*0*	*2.51154*	*3.12718*
n	*4.901202*	*4.55327*	*0*	*5.41687*	*4.90889*
o	*18.08217*	*15.0771*	*25.2565*	*45.305*	*9.13539*

4.2 Salt Phase Diagram -Model 1 n=3

1-$CaCl_2$

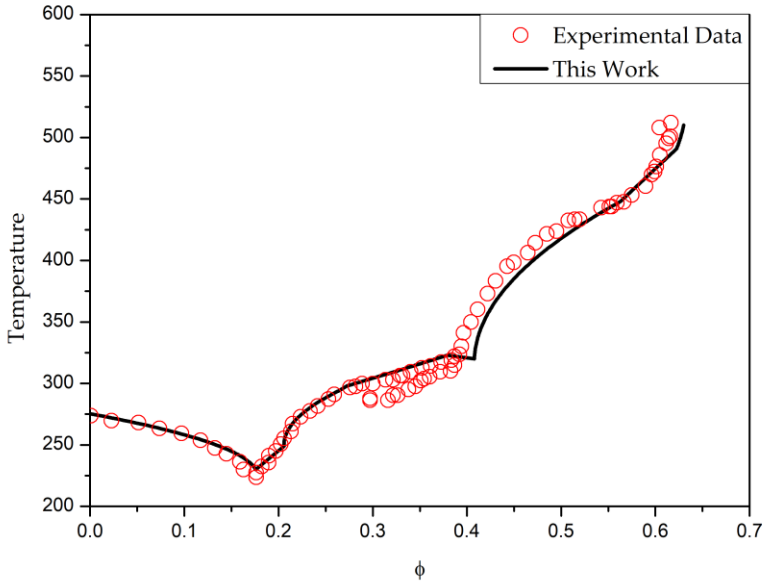

2-Li_2SO_4

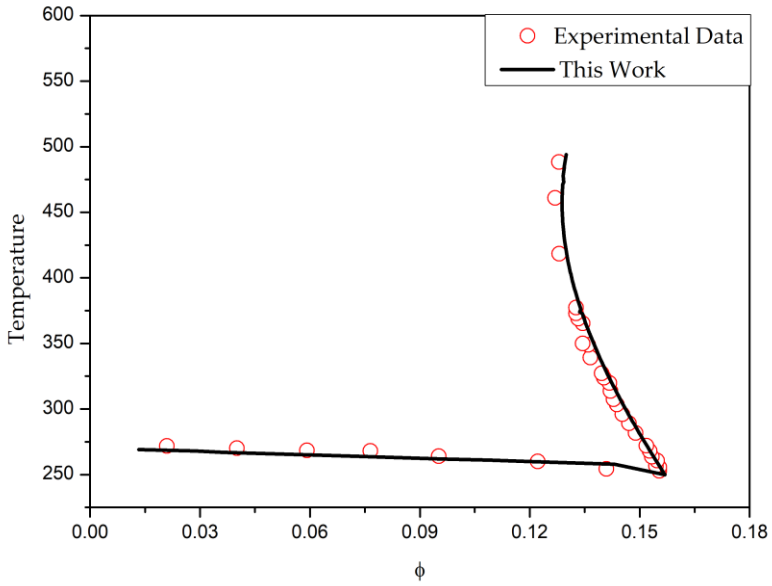

3-LiCl

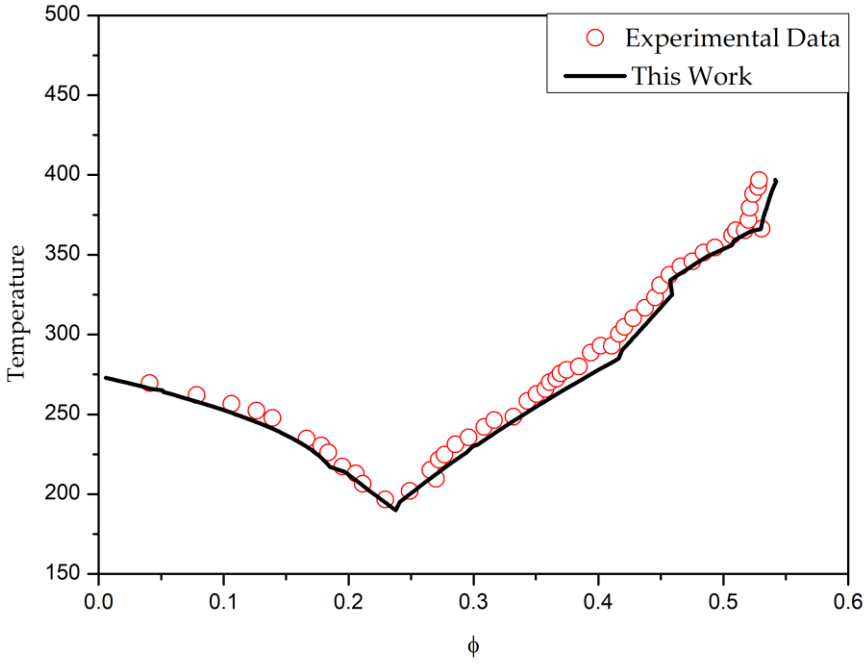
Experimental Data
This Work
Temperature
ϕ
500
450
400
350
300
250
200
150
0.0
0.1
0.2
0.3
0.4
0.5
0.6

4-NaCl

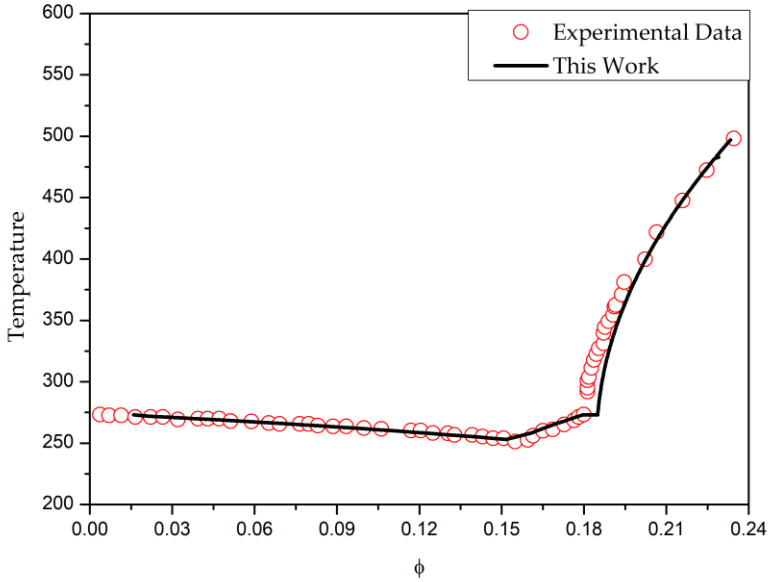
Experimental Data
This Work
Temperature
ϕ
600
550
500
450
400
350
300
250
200
0.00
0.03
0.06
0.09
0.12
0.15
0.18
0.21
0.24

5-Mg_2SO_4

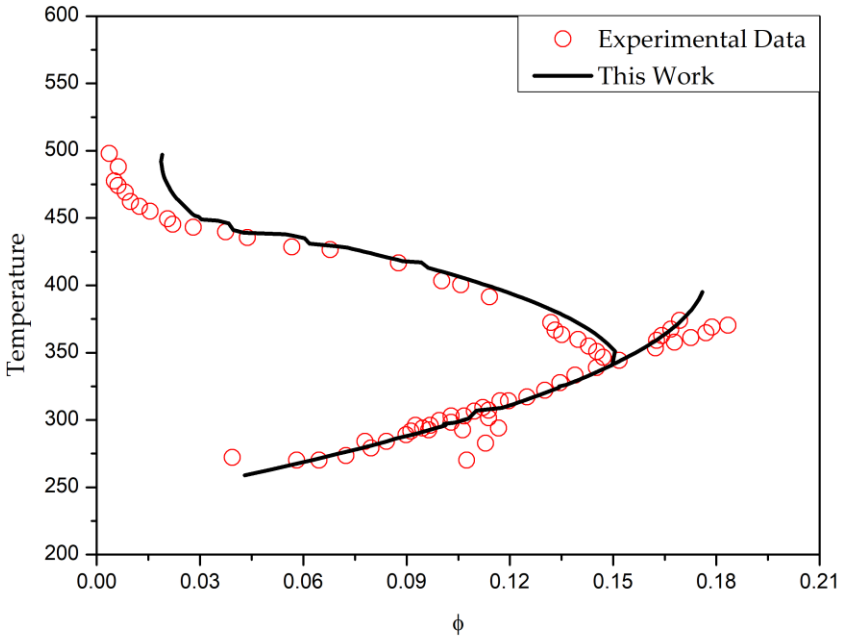

4.2 Salt Phase Diagram -Model 1 n=4

1-$CaCl_2$

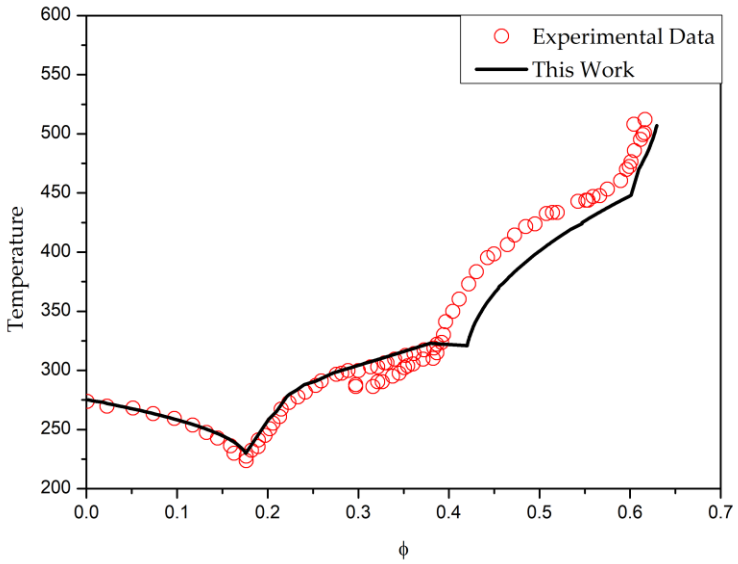

2-Li_2SO_4

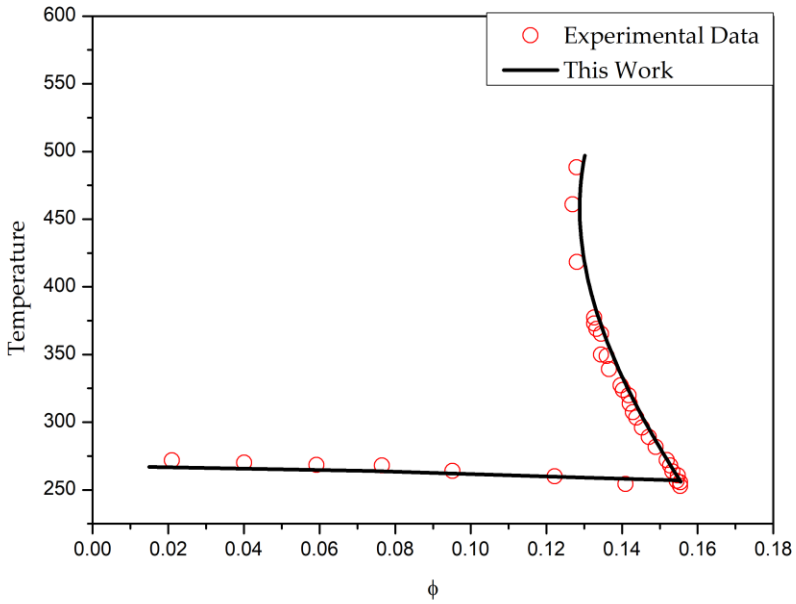

3-LiCl

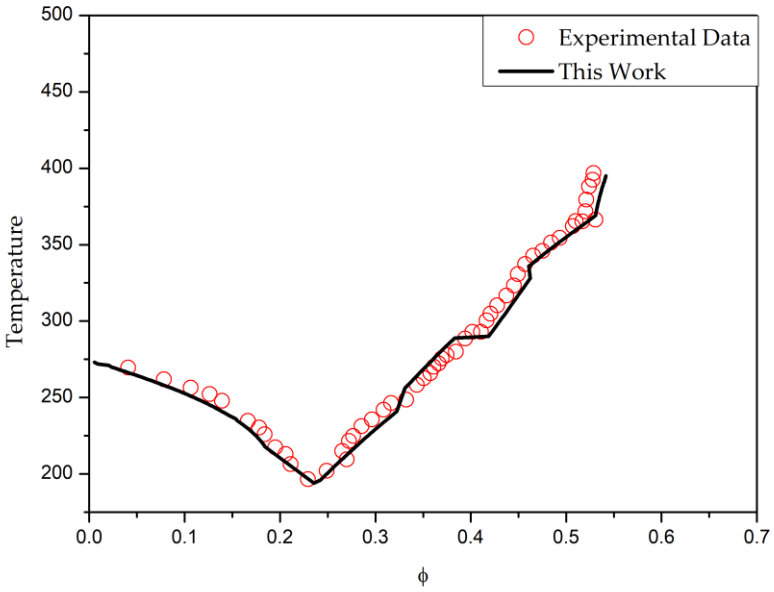

4-NaCl

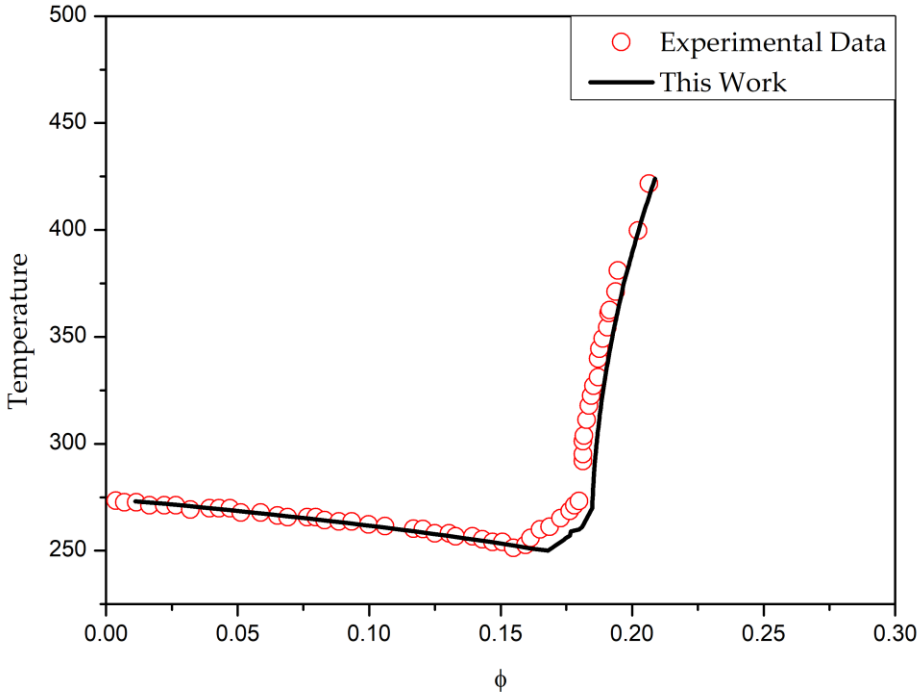

5-Mg_2SO_4

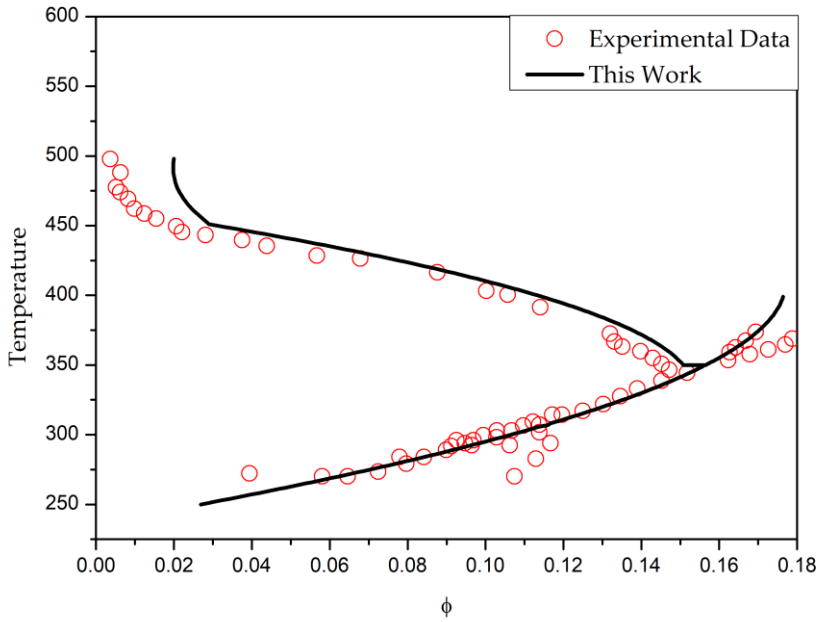

4.2 Salt Phase Diagram Model 2

1-$CaCl_2$

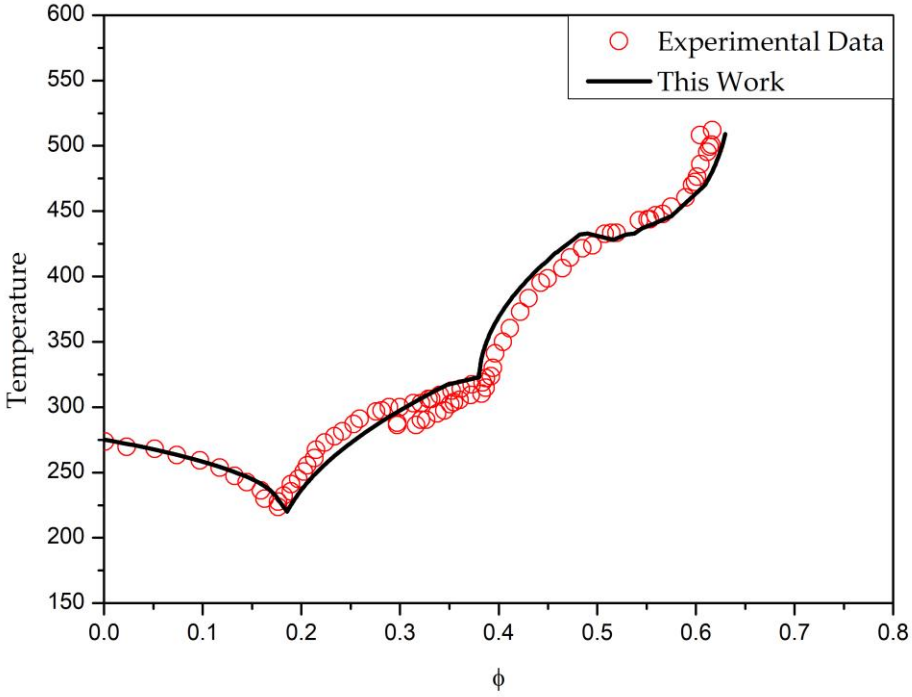

2-Li_2SO_4

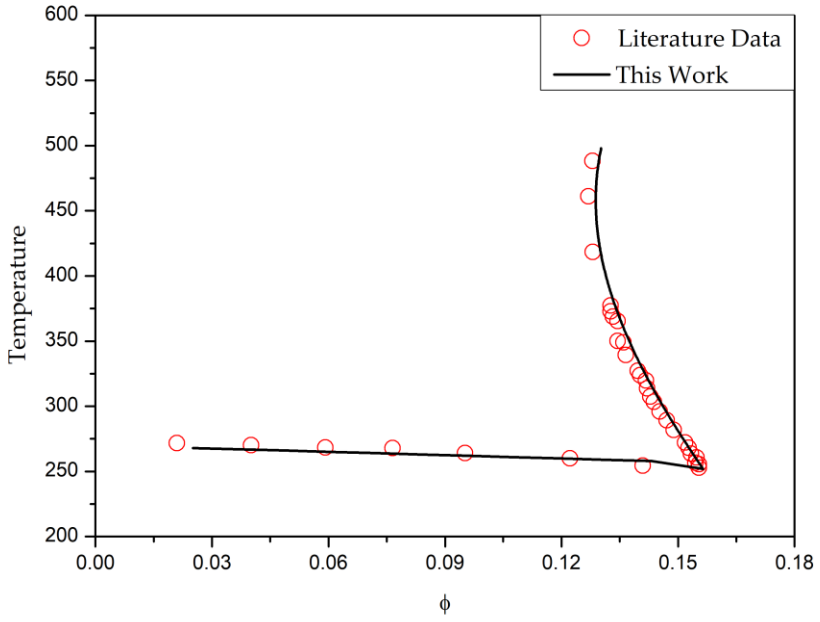

3-LiCl

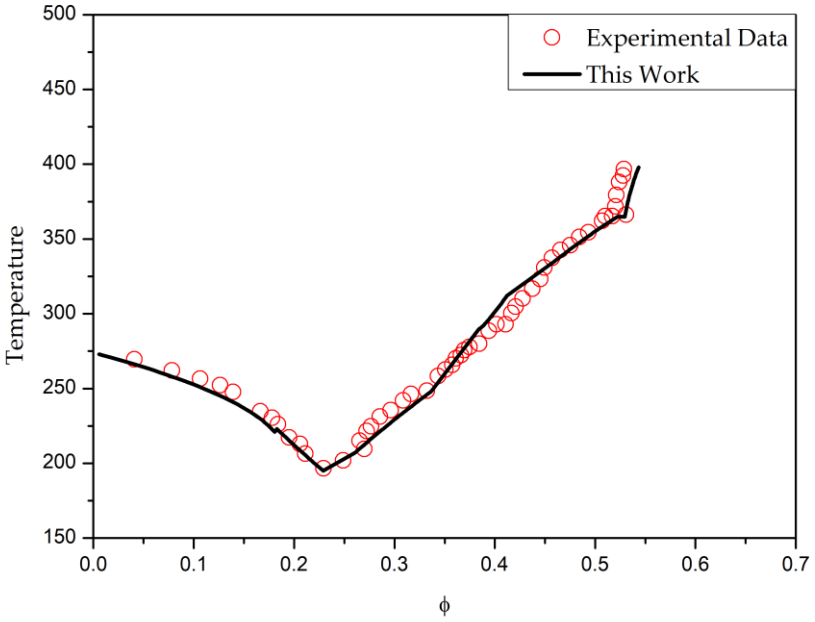
Experimental Data
This Work
Temperature
ϕ
500
450
400
350
300
250
200
150
0.0
0.1
0.2
0.3
0.4
0.5
0.6
0.7

4-NaCl

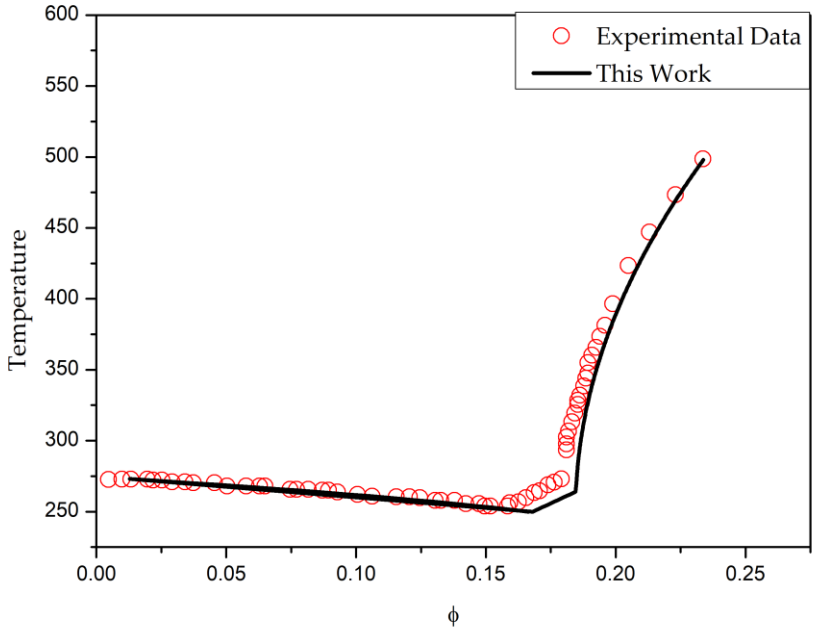
Experimental Data
This Work
Temperature
ϕ
600
550
500
450
400
350
300
250
0.00
0.05
0.10
0.15
0.20
0.25

5-Mg_2SO_4

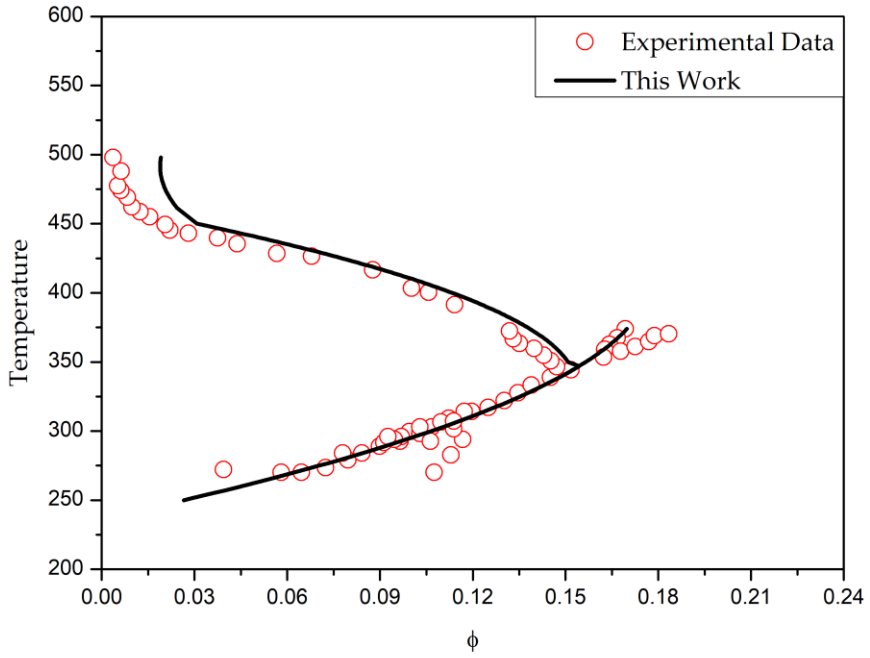
Experimental Data
This Work
Temperature
600
550
500
450
400
350
300
250
200
0.00
0.03
0.06
0.09
0.12
0.15
0.18
0.21
0.24
ϕ

CHAPTER 5

SUMMARY AND CONCLUSION

In this work, a new models is introduced to analyze the phase behavior of Salt hydrates. The present model has its limitations. Pitzer model are having a large number of parameters and the Bet model is applicable only up to a certain range, Also Deybe huckel and davies Equation deviate from the experimental result at large concentrations. The Phase Analysis Equation has been derived from the proposed model. The equations have been derived and Further steps require stimulation in Mathematica or Matlab and also validating the obtained result from literature data as well as DSC experiment.

CHAPTER 6

SCOPE FOR FUTURE WORK

Parameters and critical point are derived from the model. Phase diagram of Salts are are also modelled in this thesis. Further work can be experimented for the validation of the models.

REFERENCES

1. P.A.J. Donkers, L.C. Sögütoglu, H.P. Huinink, H.R. Fischer, O.C.G. Adan,A review of salt hydrates for seasonal heat storage in domestic applications,Applied Energy,Volume 199,2017,Pages 45-68,ISSN 0302619,https://doi.org/10.1016/j.apenergy.2017.04.080

2. A. de Jong, F. Trausel, C. Finck, L. van Vliet, R. Cuypers, Thermochemical Heat Storage – System Design Issues, Energy Procedia. 48 (2014) 309-319. doi:10.1016/j.egypro.2014.02.036.

3. L. Scapino, H. Zondag, J. Van Bael, J. Diriken, C. Rindt, Sorption heat storage for long-term low-temperature applications: A review on the advancements at material and prototype scale, Applied Energy. 190 (2017) 920-948. doi:10.1016/j.apenergy.2016.12.148.

4. D. Li, D. Zeng, X. Yin, D. Gao, Phase diagrams and thermochemical modeling of salt lake brine systems. III. Li_2SO_4+H_2O, Na_2SO_4+H_2O, K_2SO_4+H_2O, $MgSO_4$+H_2O and $CaSO_4$+H_2O systems, Calphad. 60 (2018) 163-176. doi:10.1016/j.calphad.2018.01.002.

5. F. Deyhimi, Z. Karimzadeh, Pitzer and Pitzer–Simonson–Clegg modeling approaches: Ternary HCl+1-propanol+water electrolyte system, Fluid Phase Equilibria. 287 (2010) 155-160. doi:10.1016/j.fluid.2009.10.001.

6. M. Gruszkiewicz, D. Palmer, R. Springer, P. Wang, A. Anderko, Phase Behavior of Aqueous Na–K–Mg–Ca–Cl–NO_3 Mixtures: Isopiestic Measurements and Thermodynamic Modeling, Journal Of Solution Chemistry. 36 (2007) 723-765. doi:10.1007/s10953-007-9145-2.

7. B. Ghalami-Choobar, M. Shafaghat-Lonbar, Thermodynamic investigation of the ternary mixed electrolyte (NaCl+Na_2HCit+H_2O) system using potentiometric measurements at T=(298.2 and 308.2)K, The Journal Of Chemical Thermodynamics. 78 (2014) 69-78. doi:10.1016/j.jct.2014.06.007.

8. E. Tavares, S. Marcelino, O. Chiavone-Filho, C. Souza, Determination of salt solubility data for ternary aqueous systems with a quasiisothermic thermometric technique, Thermochimica Acta. 328 (1999) 253-258. doi:10.1016/s0040-6031(98)00650-9.

9. Y. Marcus, BET Modeling of Solid–Liquid Phase Diagrams of Common Ion Binary Salt Hydrate Mixtures. I. The BET Parameters, Journal Of Solution Chemistry. 34 (2005) 297-306. doi:10.1007/s10953-005-3050-3.

10. Y. Farnam, D. Bentz, A. Sakulich, D. Flynn, J. Weiss, Measuring Freeze and Thaw Damage in Mortars Containing Deicing Salt Using a Low-Temperature Longitudinal Guarded Comparative Calorimeter and Acoustic Emission, Advances In Civil Engineering Materials. 3 (2014) 20130095. doi:10.1520/acem20130095

11. D. Li, D. Zeng, H. Han, L. Guo, X. Yin, Y. Yao, Phase diagrams and thermochemical modeling of salt lake brine systems. I. LiCl+H_2O system, Calphad. 51 (2015) 1-12. doi:10.1016/j.calphad.2015.05.001

12. T. Crivits, P. Hayes, E. Jak, An investigation of factors influencing freeze lining behaviour, Mineral Processing And Extractive Metallurgy. 127 (2017) 195-209. doi:10.1080/03719553.2017.1375767.

13. F. Elif Genceli, S. Horikawa, Y. Iizuka, T. Sakurai, T. Hondoh, T. Kawamura et al., Meridianiite detected in ice, Journal Of Glaciology. 55 (2009) 117-122. doi:10.3189/002214309788608921

14. D. Li, D. Zeng, X. Yin, D. Gao, Phase diagrams and thermochemical modeling of salt lake brine systems. III. Li_2SO_4+H_2O, Na_2SO_4+H_2O, K_2SO_4+H_2O, $MgSO_4$+H_2O and $CaSO_4$+H_2O systems, Calphad. 60 (2018) 163-176. doi:10.1016/j.calphad.2018.01.002

15. J. Pátek, J. Klomfar, Solid–liquid phase equilibrium in the systems of LiBr–H_2O and LiCl–H_2O, Fluid Phase Equilibria. 250 (2006) 138-149. doi:10.1016/j.fluid.2006.09.005.

16. F. Jiménez-Ángeles, A. Firoozabadi, Hydrophobic Hydration and the Effect of NaCl Salt in the Adsorption of Hydrocarbons and Surfactants on Clathrate Hydrates, ACS Central Science. 4 (2018) 820-831. doi:10.1021/acscentsci.8b00076.

17. N. Baird, J. Swenson, Ab initio calculations for the ground and low-lying triplet states of thioformaldehyde, The Journal Of Physical Chemistry. 77 (1973) 277-280. doi:10.1021/j100621a027.

18. W. Zhang, E. Gomez, S. Milner, Predicting Flory-Huggins χ from Simulations, Physical Review Letters. 119 (2017). doi:10.1103/physrevlett.119.017801.

19. D. Sures, G. Nagabhushana, A. Navrotsky, M. Nyman, Thermochemical Measurements of Alkali Cation Association to Hexatantalate, Molecules. 23 (2018) 2441. doi:10.3390/molecules23102441.

20. C. Rathgeber, H. Schmit, S. Hiebler, W. Voigt, Application of the modified BET model to concentrated salt solutions with relatively high water activities: Predicting solubility phase diagrams of NaCl + H_2O, NaCl + LiCl + H_2O, and NaCl + $CaCl_2$ + H_2O, Calphad. 66 (2019) 101633. doi:10.1016/j.calphad.2019.101633.

21. R. Stokes, R. Robinson, Ionic Hydration and Activity in Electrolyte Solutions, Journal Of The American Chemical Society. 70 (1948) 1870-1878. doi:10.1021/ja01185a065.

22. Y. Marcus, Unconventional Deep Eutectic Solvents: Aqueous Salt Hydrates, ACS Sustainable Chemistry & Engineering. 5 (2017) 11780-11787. doi:10.1021/acssuschemeng.7b03528.

23. M. Gruszkiewicz, J. Simonson, Vapor pressures and isopiestic molalities of concentrated $CaCl_2$(aq), $CaBr_2$(aq), and NaCl(aq) to T=523 K, The Journal Of Chemical Thermodynamics. 37 (2005) 906-930. doi:10.1016/j.jct.2004.12.009.

24. 1] D. Zeng, J. Ming, W. Voigt, Thermodynamic study of the system (LiCl+$LiNO_3$+H_2O), The Journal Of Chemical Thermodynamics. 40 (2008) 232-239. doi:10.1016/j.jct.2007.06.018.

25. V. Brendler, W. Voigt, Isopiestic measurements at high temperatures: I. Aqueous solutions of LiCl, CsCl, and $CaCl_2$ at 155^0C, Journal Of Solution Chemistry. 23 (1994) 1061-1072. doi:10.1007/bf00976256.

26. H. Gibbard, G. Scatchard, Liquid-vapor equilibrium of aqueous lithium chloride, from 25 to 100.deg. and from 1.0 to 18.5 molal, and related properties, Journal Of Chemical & Engineering Data. 18 (1973) 293-298. doi:10.1021/je60058a011.

27. H. Gibbard, A. Fawaz, Freezing points and related properties of electrolyte solutions. II. Mixtures of lithium chloride and sodium chloride in water, Journal Of Solution Chemistry. 3 (1974) 745-755. doi:10.1007/bf00955707.

28. H. Holmes, R. Mesmer, Thermodynamic properties of aqueous solutions of the alkali metal chlorides to 250.degree.C, The Journal Of Physical Chemistry. 87 (1983) 1242-1255. doi:10.1021/j100230a030.

29. A. Campbell, J. Griffiths, THE SYSTEM LITHIUM CHLORATE – LITHIUM CHLORIDE – WATER AT VARIOUS TEMPERATURES, Canadian Journal Of Chemistry. 34 (1956) 1647-1661. doi:10.1139/v56-213.

30. R. Song, T. Zou, J. Chen, X. Hou, X. Han, Study on the Physical Properties of LiCl Solution, IOP Conference Series: Materials Science And Engineering. 562 (2019) 012102. doi:10.1088/1757-899x/562/1/012102.

31. X. Ma, W. Shen, X. Li, Y. Hu, X. Liu, X. Lu, Experimental investigation on water adsorption and desorption isotherms of the Longmaxi shale in the Sichuan Basin, China, Scientific Reports. 10 (2020). doi:10.1038/s41598-020-70222-8.

32. Ren, Qian, Yao, Gan, Zhang, Thermodynamic Evaluation of LiCl-H_2O and LiBr-H_2O Absorption Refrigeration Systems Based on a Novel Model and Algorithm, Energies. 12 (2019) 3037. doi:10.3390/en12153037.

33. H. Braunstein, J. Braunstein, Isopiestic studies of very concentrated aqueous electrolyte solutions of LiCl, LiBr, $LiNO_3$, $Ca(NO_3)_2$, $LiNO_3$ + KNO_3, $LiNO_3$ + $CsNO_3$, and $Ca(NO_3)_2$ + $CsNO_3$ at 100 to 150°C, The Journal Of Chemical Thermodynamics. 3 (1971) 419-431. doi:10.1016/s0021-9614(71)80025-3.

34. H. Rammelberg, T. Schmidt, W. Ruck, Hydration and dehydration of salt hydrates and hydroxides for thermal energy storage - kinetics and energy release, Energy Procedia. 30 (2012) 362-369. doi:10.1016/j.egypro.2012.11.043.

35. J. Rard, S. Clegg, D. Palmer, Isopiestic Determination of the Osmotic and Activity Coefficients of Li_2SO_4(aq) at T=298.15 and 323.15 K, and Representation with an Extended Ion-Interaction (Pitzer) Model, Journal Of Solution Chemistry. 36 (2007) 1347-1371. doi:10.1007/s10953-007-9190-x.

36. R. Goldberg, Evaluated activity and osmotic coefficients for aqueous solutions: thirty-six uni-bivalent electrolytes, Journal Of Physical And Chemical Reference Data. 10 (1981) 671-764. doi:10.1063/1.555646.

37. J. Rard, D. Miller, Isopiestic determination of the osmotic and activity coefficients of aqueous mixtures of sodium chloride and strontium chloride at 25.0^{0}C, Journal Of Chemical & Engineering Data. 27 (1982) 342-346. doi:10.1021/je00029a033.

38. J. Zhang, D. Li, Y. Yao, B. Sun, D. Zeng, P. Song, Thermodynamic Properties of LiCl + $MgSO_4$ + H_2O at Temperatures from 273.15 K to 373.15 K and Representation with Pitzer Ion-Interaction Model, Journal Of Chemical & Engineering Data. 61 (2016) 2277-2291. doi:10.1021/acs.jced.5b00987.

39. R. Platford, Osmotic coefficients of aqueous solutions of seven compounds at 0.deg., Journal Of Chemical & Engineering Data. 18 (1973) 215-217. doi:10.1021/je60057a017.

40. M. Guendouzi, A. Mounir, A. Dinane, Water activity, osmotic and activity coefficients of aqueous solutions of Li2SO4, Na2SO4, K2SO4, (NH4)2SO4, MgSO4, MnSO4, NiSO4, CuSO4, and ZnSO4 at T=298.15K, The Journal Of Chemical Thermodynamics. 35 (2003) 209-220. doi:10.1016/s0021-9614(02)00315-4.

41. D. Zeng, J. Zhou, Thermodynamic Consistency of the Solubility and Vapor Pressure of a Binary Saturated Salt + Water System. Part 1. LiCl + H_2O, Cheminform. 37 (2006). doi:10.1002/chin.200621224.

42. X. Xu, Z. Dong, S. Memon, X. Bao, H. Cui, Preparation and Supercooling Modification of Salt Hydrate Phase Change Materials Based on $CaCl_2$·2H2O/$CaCl_2$, Materials. 10 (2017) 691. doi:10.3390/ma10070691.

43. M. Ally, Predicting phase diagram of the $CaCl_2$·H_2O binary system from the BET adsorption isotherm, Fluid Phase Equilibria. 268 (2008) 45-50. doi:10.1016/j.fluid.2008.03.017.

44. X. Xu, Z. Dong, S. Memon, X. Bao, H. Cui, Preparation and Supercooling Modification of Salt Hydrate Phase Change Materials Based on $CaCl_2$·2H_2O/$CaCl_2$, Materials. 10 (2017) 691. doi:10.3390/ma10070691.

45. C. Monnin, M. Dubois, N. Papaiconomou, J. Simonin, Thermodynamics of the LiCl + H_2O System, Journal Of Chemical & Engineering Data. 47 (2002) 1331-1336. doi:10.1021/je0200618.

46. A. de Jong, L. van Vliet, C. Hoegaerts, M. Roelands, R. Cuypers, Thermochemical Heat Storage – from Reaction Storage Density to System Storage Density, Energy Procedia. 91 (2016) 128-137. doi:10.1016/j.egypro.2016.06.187.

47. K. N'Tsoukpoe, T. Schmidt, H. Rammelberg, B. Watts, W. Ruck, A systematic multi-step screening of numerous salt hydrates for low temperature thermochemical energy storage, Applied Energy. 124 (2014) 1-16. doi:10.1016/j.apenergy.2014.02.053.

48. M. Graham, E. Shchukina, P. De Castro, D. Shchukin, Nanocapsules containing salt hydrate phase change materials for thermal energy storage, Journal Of Materials Chemistry A. 4 (2016) 16906-16912. doi:10.1039/c6ta06189c.

49. L. Liang, X. Chen, Preparation and Thermal Properties of Eutectic Hydrate Salt Phase Change Thermal Energy Storage Material, International Journal Of Photoenergy. 2018 (2018) 1-9. doi:10.1155/2018/6432047.

50. L. Scapino, H. Zondag, J. Van Bael, J. Diriken, C. Rindt, Sorption heat storage for long-term low-temperature applications: A review on the advancements at material and prototype scale, Applied Energy. 190 (2017) 920-948. doi:10.1016/j.apenergy.2016.12.148.

51. H. Yang, H. Cui, W. Fung, T. Lo, Excellent Thermophysical Properties of Salt Hydrate Phase-Change Material for Thermal Storage Systems, SSRN Electronic Journal. (2021). doi:10.2139/ssrn.3892698.

52. M. Gaeini, A. Rouws, J. Salari, H. Zondag, C. Rindt, Characterization of microencapsulated and impregnated porous host materials based on calcium chloride for thermochemical energy storage, Applied Energy. 212 (2018) 1165-1177. doi:10.1016/j.apenergy.2017.12.131.

53. W. Viola, T. Andrew, An Aqueous Eutectic Electrolyte for Low-Cost, Safe Energy Storage with an Operational Temperature Range of 150 °C, from −70 to 80 °C, The Journal Of Physical Chemistry C. 125 (2020) 246-251. doi:10.1021/acs.jpcc.0c09676.

54. Z. Wang, X. Li, S. Sang, X. Ma, Mean Activity Coefficients of NaCl in the NaCl–SrCl2–H_2O Ternary System at 308 K by EMF Method, Journal Of Chemical & Engineering Data. 64 (2019) 442-447. doi:10.1021/acs.jced.8b00491.

55. F. Farelo, C. Fernandes, A. Avelino, Solubilities for Six Ternary Systems: NaCl + NH4Cl + H_2O, KCl + NH_4Cl + H_2O, NaCl + LiCl + H_2O, KCl + LiCl + H_2O, NaCl + $AlCl_3$ + H_2O, and KCl + $AlCl_3$ + H2O at T = (298 to 333) K., Cheminform. 36 (2005). doi:10.1002/chin.200540019.

56. B. Lü, The correlation of activity coefficients for the electrolyte-nonelectrolyte mixed solution -the thermodynamics of the liquid solid phase equilibria in (NH2)2CO-NaCl-NH4Cl-H2O system, Acta Chimica Sinica. 4 (1986) 283-293. doi:10.1002/cjoc.19860040402.

57. H. Galleguillos, T. Graber, M. Taboada, F. Hernández-Luis, Activity coefficients of NaCl in the NaCl+NaBF4+H2O ternary system at 298.15K, Fluid Phase Equilibria. 275 (2009) 39-45. doi:10.1016/j.fluid.2008.09.015.

58. C. Venkateswarlu, J. Ananthaswamy, Thermodynamics of electrolyte solutions: activity coefficients of NaCl in the NaCl–NiCl2–H_2O system at 25, 35, and 45 °C, Canadian Journal Of Chemistry. 68 (1990) 294-297. doi:10.1139/v90-040.

59. M. Wang, H. Zhang, J. Wang, Z. Wang, Isopiestic studies on the saturated systems {H2O+$BaCl_2$(sat)+NaCl+NH_4Cl} and {H2O+$BaCl_2$(sat)+mannitol(sat)+NaCl+NH_4Cl} at the temperature 298.15K: Comparison with the ideal-like solution model, The Journal Of Chemical Thermodynamics. 39 (2007) 316-321. doi:10.1016/j.jct.2006.06.011.

60. R. Robinson, H. McCoach, Osmotic and Activity Coefficients of Lithium Bromide and Calcium Bromide Solutions, Journal Of The American Chemical Society. 69 (1947) 2244-2244. doi:10.1021/ja01201a517.

61. A. Covington, D. Irish, Osmotic and activity coefficients of aqueous ammonium bromide solutions at 25.deg., Journal Of Chemical & Engineering Data. 17 (1972) 175-176. doi:10.1021/je60053a034.

62. A. Usha, K. Raju, G. Atkinson, Thermodynamics of concentrated electrolyte mixtures. Activity coefficients in aqueous sodium bromide-calcium bromide mixtures at 250C, The Journal Of Physical Chemistry. 91 (1987) 4796-4799. doi:10.1021/j100302a029.

63. D. Zeng, W. Voigt, Phase diagram calculation of molten salt hydrates using the modified BET equation, Calphad. 27 (2003) 243-251. doi:10.1016/j.calphad.2003.09.004.

64. H. Naidu, A. Virkar, Low-Temperature TiO2-SnO2 Phase Diagram Using the Molten-Salt Method, Journal Of The American Ceramic Society. 81 (2005) 2176-2180. doi:10.1111/j.1151-2916.1998.tb02603.x.

65. H. Emons, Structure and properties of molten salt hydrates, Electrochimica Acta. 33 (1988) 1243-1250. doi:10.1016/0013-4686(88)80155-5.

66. Y. Marcus, BET Modeling of Solid–Liquid Phase Diagrams of Common-Ion Binary Salt Hydrate Mixtures. II. Calculation of Liquidus Temperatures, Journal Of Solution Chemistry. 34 (2005) 307-315. doi:10.1007/s10953-005-3051-2.

67. G. Gözaydın, S. Song, N. Yan, Chitin hydrolysis in acidified molten salt hydrates, Green Chemistry. 22 (2020) 5096-5104. doi:10.1039/d0gc01464h.

68. Y. Marcus, Volumetric Properties of Molten Salt Hydrates, Journal Of Chemical & Engineering Data. 58 (2013) 488-491. doi:10.1021/je301277p.

69. Y. Ding, N. Gao, Y. Wu, Y. Xuan, G. Chen, Vapor-Pressure Measurement of Ternary System $CaCl_2$ + Br + H_2O, $CaCl_2$ + Cl + H_2O, $CaCl_2$ + Ac + H_2O, and $CaCl_2$ + NO_3 + H_2O, Journal Of Chemical & Engineering Data. 66 (2020) 692-701. doi:10.1021/acs.jced.0c00829.

70. D. Jaques, W. Furter, Salt effects in vapor-liquid equilibrium: Testing the thermodynamic consistency of ethanol-water saturated with inorganic salts, Aiche Journal. 18 (1972) 343-346. doi:10.1002/aic.690180216.

71. W. Lightfoot, C. Prutton, Equilibria in Saturated Salt Solutions. II. The Ternary Systems $CaCl_2$-$MgCl_2$-H_2O, CaCl2-KCl-H_2O and $MgCl_2$-KCl-H_2O at 75°, Journal Of The American Chemical Society. 69 (1947) 2098-2100. doi:10.1021/ja01201a005.

72. A. Konyshev, A. Aksyuk, V. Korzhinskaya, Quartz Solubility in the Vapor Phase of the H_2O–HF System at 200°C and Saturated Vapor Pressure: Experimental Data, Geochemistry International. 56 (2018) 1109-1115. doi:10.1134/s0016702918110058.

73. A. Lach, L. André, A. Lassin, M. Azaroual, J. Serin, P. Cézac, A New Pitzer Parameterization for the Binary NaOH–H2O and Ternary NaOH–NaCl–H_2O and NaOH–LiOH–H_2O Systems up to NaOH Solid Salt Saturation, from 273.15 to 523.15 K and at Saturated Vapor Pressure, Journal Of Solution Chemistry. 44 (2015) 1424-1451. doi:10.1007/s10953-015-0357-6.

74. W. Lightfoot, C. Prutton, Equilibria in Saturated Salt Solutions. IV. The Quaternary System $CaCl_2$--$MgCl_2$--KCl--H_2O at 75°, Journal Of The American Chemical Society. 71 (1949) 1233-1235. doi:10.1021/ja01172a027.

75. I. Igelsrud, T. Thompson, Equilibria in the Saturated Solutions of Salts Occurring in Sea Water. II. The Quaternary System $MgCl_2$-$CaCl_2$-KCl-H_2O at 0°, Journal Of The American Chemical Society. 58 (1936) 2003-2009. doi:10.1021/ja01301a053.

76. L. Guo, D. Zeng, Y. Yao, H. Han, Isopiestic measurement and solubility evaluation of the ternary system ($CaCl_2$+$SrCl_2$+H_2O) at T=298.15K, The Journal Of Chemical Thermodynamics. 63 (2013) 60-66. doi:10.1016/j.jct.2013.03.021.

77. J. Fu, Salt effect on vapor–liquid equilibria for binary systems of propanol/$CaCl_2$ and butanol/$CaCl_2$, Fluid Phase Equilibria. 237 (2005) 219-223. doi:10.1016/j.fluid.2005.07.023.

78. C. Che, Y. Yin, A statistical thermodynamic model for prediction of vapor pressure of mixed liquid desiccants near saturated solubility, Energy. 175 (2019) 798-809. doi:10.1016/j.energy.2019.03.115.

79. Z. Bakher, M. Kaddami, Thermodynamic equilibrium study of phosphorus pentoxide-water binary system: The stability and solubility of 10H3PO4.H2O, Calphad. 63 (2018) 148-155. doi:10.1016/j.calphad.2018.09.006.

80. D. Platte, U. Helbig, R. Houbertz, G. Sextl, Microencapsulation of Alkaline Salt Hydrate Melts for Phase Change Applications by Surface Thiol-Michael Addition Polymerization, Macromolecular Materials And Engineering. 298 (2012) 67-77. doi:10.1002/mame.201100338.

81. N. Kumar, R. Ness, R. Chavez, D. Banerjee, A. Muley, M. Stoia, Experimental Analysis of Salt Hydrate Latent Heat Thermal Energy Storage System With Porous Aluminum Fabric and Salt Hydrate as Phase Change Material With Enhanced Stability and Supercooling, Journal Of Energy Resources Technology. 143 (2020). doi:10.1115/1.4048122.

82. A. Mehrabadi, M. Farid, New salt hydrate composite for low-grade thermal energy storage, Energy. 164 (2018) 194-203. doi:10.1016/j.energy.2018.08.192.

83. S. Hamad, An experimental study of the salt hydrate $MgSO_4 \cdot 7H_2O$, Thermochimica Acta. 13 (1975) 409-418. doi:10.1016/0040-6031(75)85082-9.

84. A. Mohammadi, D. Richon, Thermodynamic Modeling of Salt Precipitation and Gas Hydrate Inhibition Effect of Salt Aqueous Solution, Industrial & Engineering Chemistry Research. 46 (2007) 5074-5079. doi:10.1021/ie061686s.

85. L. Feng, B. Tian, B. Wang, M. Yang, Purification of hydrazine hydrate waste salt using a water washing based integrated process for the production of sodium hydrate via ion-exchange membrane electrolysis, Journal Of Cleaner Production. 319 (2021) 128626. doi:10.1016/j.jclepro.2021.128626.

86. B. Purohit, V. Sistla, Inorganic salt hydrate for thermal energy storage application: A review, Energy Storage. 3 (2020). doi:10.1002/est2.212.

87. B. Topley, M. Smith, 69. Kinetics of salt-hydrate dissociations: MnC_2O_4,$2H_2O$ = MnC2O_4+ $2H_2O$, Journal Of The Chemical Society (Resumed). (1935) 321. doi:10.1039/jr9350000321.

88. E. Tieger, V. Kiss, G. Pokol, Z. Finta, Crystallisation of a salt hydrate with a complex solid form landscape, Crystengcomm. 19 (2017) 1912-1925. doi:10.1039/c7ce00041c.

89. J. Duffy, G. Wood, Molten-salt hydrate media. Cobalt(II) ions in $ZnCl_2$+ H_2O and $CaCl_2$+ H_2O systems, Journal Of The Chemical Society, Faraday Transactions 1: Physical Chemistry In Condensed Phases. 81 (1985) 265. doi:10.1039/f19858100265.

90. G. Li, B. Zhang, X. Li, Y. Zhou, Q. Sun, Q. Yun, The preparation, characterization and modification of a new phase change material: CaCl2·6H2O–MgCl2·6H2O eutectic hydrate salt, Solar Energy Materials And Solar Cells. 126 (2014) 51-55. doi:10.1016/j.solmat.2014.03.031.

91. J. Fu, Salt effect on vapor–liquid equilibria for binary systems of propanol/$CaCl_2$ and butanol/$CaCl_2$, Fluid Phase Equilibria. 237 (2005) 219-223. doi:10.1016/j.fluid.2005.07.023.

92. K. Meisingset, F. Grønvold, Thermodynamic properties and phase transitions of salt hydrates between 270 and 400 K IV. $CaCl_2·6H_2O$, $CaCl_2·4H_2O$, CaCl2·2H_2O, and $FeCl_3·6H_2O$, The Journal Of Chemical Thermodynamics. 18 (1986) 159-173. doi:10.1016/0021-9614(86)90130-8.

93. M. Baumgartner, R. Bakker, $CaCl_2$-hydrate nucleation in synthetic fluid inclusions, Chemical Geology. 265 (2009) 335-344. doi:10.1016/j.chemgeo.2009.04.012.

94. Y. Liu, H. Huang, R. Tang, L. Han, J. Yang, M. Xu et al., NMR study on the cellulose dissolution mechanism in $CaCl_2·6H_2O$–LiCl molten salt hydrate, Physical Chemistry Chemical Physics. 23 (2021) 20489-20495. doi:10.1039/d1cp02769g.

95. A. Chialvo, The effect of salt concentration on the structure of water in $CaCl_2$ aqueous solutions, Journal Of Molecular Liquids. (2004). doi:10.1016/s0167-7322(03)00267-8.

96. Z. Long, L. Zha, D. Liang, D. Li, Phase Equilibria of CO2 Hydrate in $CaCl_2$–$MgCl_2$ Aqueous Solutions, Journal Of Chemical & Engineering Data. 59 (2014) 2630-2633. doi:10.1021/je500400s.

97. W. Wendlandt, The detection of quadruple points in metal salt hydrate systems by electrical conductivity measurements, Thermochimica Acta. 1 (1970) 11-17. doi:10.1016/0040-6031(70)85024-9.

98. S. Deki, Melting Behavior for Powders/Hydrate Melt ($CaCl_2·nH_2O$; n=6.00, 7.35) Coexisting Systems, ECS Proceedings Volumes. 1992-16 (1992) 586-594. doi:10.1149/199216.0586pv

99. P. Donkers, L. Pel, O. Adan, Experimental studies for the cyclability of salt hydrates for thermochemical heat storage, Journal Of Energy Storage. 5 (2016) 25-32. doi:10.1016/j.est.2015.11.005.

100. B. Purohit, V. Sistla, Inorganic salt hydrate for thermal energy storage application: A review, Energy Storage. 3 (2020). doi:10.1002/est2.212.

101. M. Zbair, S. Bennici, Survey Summary on Salts Hydrates and Composites Used in Thermochemical Sorption Heat Storage: A Review, Energies. 14 (2021) 3105. doi:10.3390/en14113105.

102. H. Wang, Y. Chen, J. Li, L. Guo, M. Fang, Review of Encapsulated Salt Hydrate Core-Shell Phase Change Materials, KONA Powder And Particle Journal. 37 (2020) 85-96. doi:10.14356/kona.2020010.